journal of the

INTERNATIONAL SOCIETY for PLASTINATION

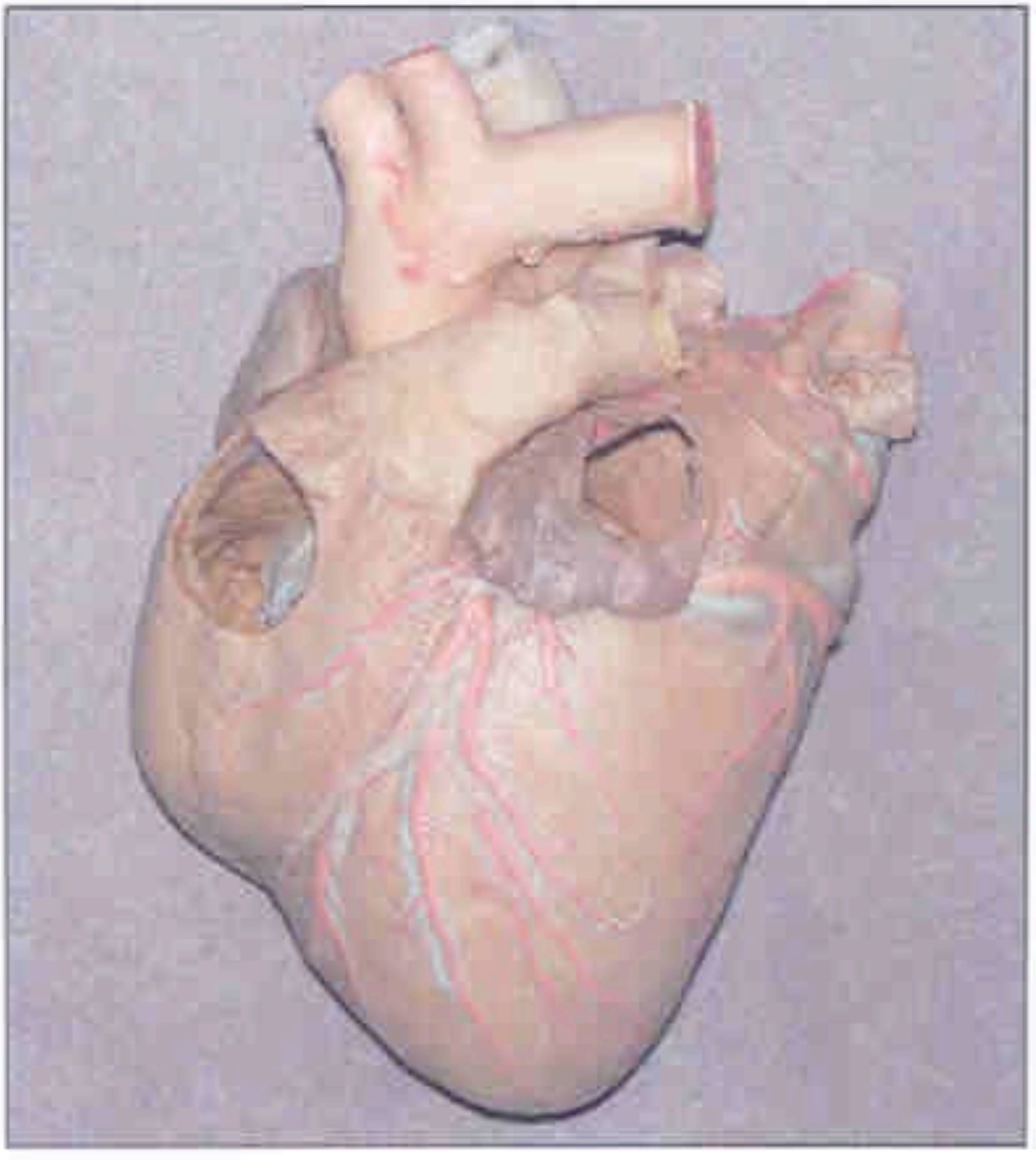

Volume 18
Fall 2003

Journal of the International Society **for** Plastination **18:3-8** (2003)

Effects of Reduced Pressure on Components of Epoxy (E12) Reaction Mixture

R.B. REED*

Department of Comparative Medicine, College of Veterinary Medicine, University of Tennessee, 2407 River Drive, Knoxville, 77V, *37996, USA.*

Correspondence to: Telephone: 865 - 974 - 5823; *Fax:* 865 - 974 - 5640; *E-mail:* rbreed@utk.edu

Abstract: To determine the effects of reduced pressure on the reaction mixture used in epoxy plastination, the components of this process, both individually and in combination, were exposed to a reduced pressure within a vacuum chamber. Production of bubbles within the reaction mixture components occurred at three different points during the experiment. The first generation of bubbles appeared with a slight decrease in pressure and most likely came from air trapped in the mixtures. The second generation of bubbles appeared when the manometer reached 10.3cm of Hg. These bubbles were released from the epoxy polymer (El2). The third generation of bubbles appeared when the manometer reached 1.0cm of Hg. These bubbles were released from the epoxy hardener (El). Release of these components of the epoxy reaction mixture does not affect their ability to cure.

Key words: epoxy; **plastination; vacuum**

Introduction

Plastination of biological tissue with epoxy polymer is a unique method by which to preserve thin slices of tissue. These tissue slices may be used for teaching or research purposes (Guhr et al., 1987; Cook, 1997a; Cook 1997b; Phillips et al., 2002). The epoxy in which the specimens are preserved should be as free of artifacts as possible to enhance their usefulness to education or medical investigations. Some of the difficulties plastinators encounter when using epoxy polymer have been reported (Mathura, 1996; Weber and Henry, 1993). One artifact which commonly appears in epoxy plastinated sheets of tissue is the presence of bubbles. Air is introduced into the epoxy reaction mixture during mixing or during filling of casting chambers. Air bubbles may be removed from reaction filled casting chambers by increasing external pressure on the sides of the casting chamber (Guhr et al., 1987), teasing them out with a probe (von Hagens, 1985; Weber and Henry, 1993; Latorre et al., 2002) or drawing them out under vacuum (Weber and Henry, 1993; Skalkos et al., 1999; Latorre et al., 2002). When using the vacuum method, the reduction in pressure often appears to increase the number of bubbles in the reaction mixture. Initially, gas bubbles are removed from the casting chamber when pressure is decreased. This is followed by the manifestation of many pinpoint size bubbles which often increase in number to the point of producing a foam on the surface of the reaction mixture (Latorre et al., 2002). It is possible that decreased pressure does not just pull air from the epoxy but is also capable of removing some component of the polymer, in a gaseous form, from the reaction mixture. This study evaluated the components of epoxy plastination individually and in combination under vacuum in an attempt to establish the source of the additional bubbles.

Materials and methods

The components of epoxy (El2) plastination were mixed at 95 parts of polymer to 26 parts of hardener to 5 parts of glass separator by weight (von Hagens, 1989). The experimental reaction mixtures were as follows: mixture 1 - El alone, mixture 2 - El2 alone, mixture 3 - AE30 alone, mixture 4 - El and El2, mixture 5 - El and AE30, mixture 6 - El2 and AE30, mixture 7 - El, E12 and AE30. Each test combination was poured into 50ml glass beakers and stirred gently to avoid the introduction of excess air. Each mixture combination was produced in triplicate. The beakers and contents were placed into a vacuum chamber and the pressure was gradually decreased. Pressure was initially measured with a pressure gauge and subsequently measured with a manometer as the vacuum increased (Henry and Thompson, 1992). The experiment was conducted at room temperature (22-23°C). The contents of the beakers were monitored for production of bubbles throughout the experiment. All beakers were left in the vacuum chamber until the point that bubble production ceased in all beakers. Mixtures were evaluated 2, 30 and 180 days following completion of the experiment to assess curing and appearance of the final products.

Results

The beaker containing glass separator never showed bubble formation throughout the duration of the experiment. The level of glass separator in the beaker decreased gradually over time and had entirely evaporated within 12 hours.

All other combinations of reaction mixture components showed generation of small bubbles with an approximate diameter of 0.5mm or less when gauge pressure measured between 12.5 and 15.0cm Hg (Table 1). The beakers containing polymer alone and polymer with glass separator both produced bubbles of 0.5mm or less in diameter at 12.5cm Hg on the gauge. The beaker containing only hardener showed a generation of these same sized bubbles at 14.2cm Hg on the gauge. The beaker containing hardener with polymer showed generation of these bubbles at 15.0cm Hg on the gauge. The beaker containing hardener with separator as well as the beaker containing all three components showed bubble production so slight that it could almost be considered negligible. These small diameter bubbles persisted in the beakers, clustered around the surface of the liquids, without much change until larger bubbles were later generated which obliterated them. These initial bubbles were not captured photographically due to their extremely small size combined with the difficulties involved in photographing the beakers through the thick glass cover of the vacuum chamber.

When the manometer reached 10.3cm Hg, all four beakers containing epoxy polymer began to produce bubbles measuring from 3.0 to 12.0mm in diameter (Table 2) (Figs. IB, 1C, IE, IF). The two beakers in which the polymer and hardener were combined produced bubbles vigorously at 10.3cm Hg (Figs. 1C, IF). A few bubbles were generated in the beaker containing El combined with AE30, however these bubbles appeared only occasionally and remained present at the surface as they were not disrupted (Fig. ID). No bubble production occurred in the beaker containing El alone (Fig. 1A).

At 1.0cm Hg, the beakers containing only hardener and hardener with glass separator began to produce bubbles measuring from 2.0 - 3.0mm in diameter (Table 2) (Figs. 2A, 2D). The four beakers containing polymer continued to produce bubbles at 1.0cm Hg (Figs. 2B, 2C, 2E, 2F). The beakers containing polymer alone and polymer with hardener exhibited a marked production of gas bubbles at 1.0cm Hg (Figs. 2B, 2C).

El	14.2 cm Hg
E12	12.5 cm Hg
AE30	-
E1 + E12	15.0 cm Hg
El + AE30	-
E12+AE30	12.5 cm Hg
E1+E12+AE30	-

Table 1. Pressure at which air bubble formation was induced in reaction mixture components.

El	l.0cmHg
E12	10.3 cm Hg
AE30	-
E1+E12	10.3 cm Hg
El + AE30	l.0cmHg
E12+AE30	10.3 cm Hg
E1+E12+AE30	10.3 cm Hg

Table 2. Pressure at which a component of experimental reaction mixtures first began to be released in a gaseous form.

Bubble production in the six beakers continued to the point of greatest vacuum which was 0.7cm Hg. Bubble production continued in the contents of the beakers until they gradually began to taper off between 18 and 24 hours after the experiment began. Twenty-four hours after the start of the experiment, all bubble production

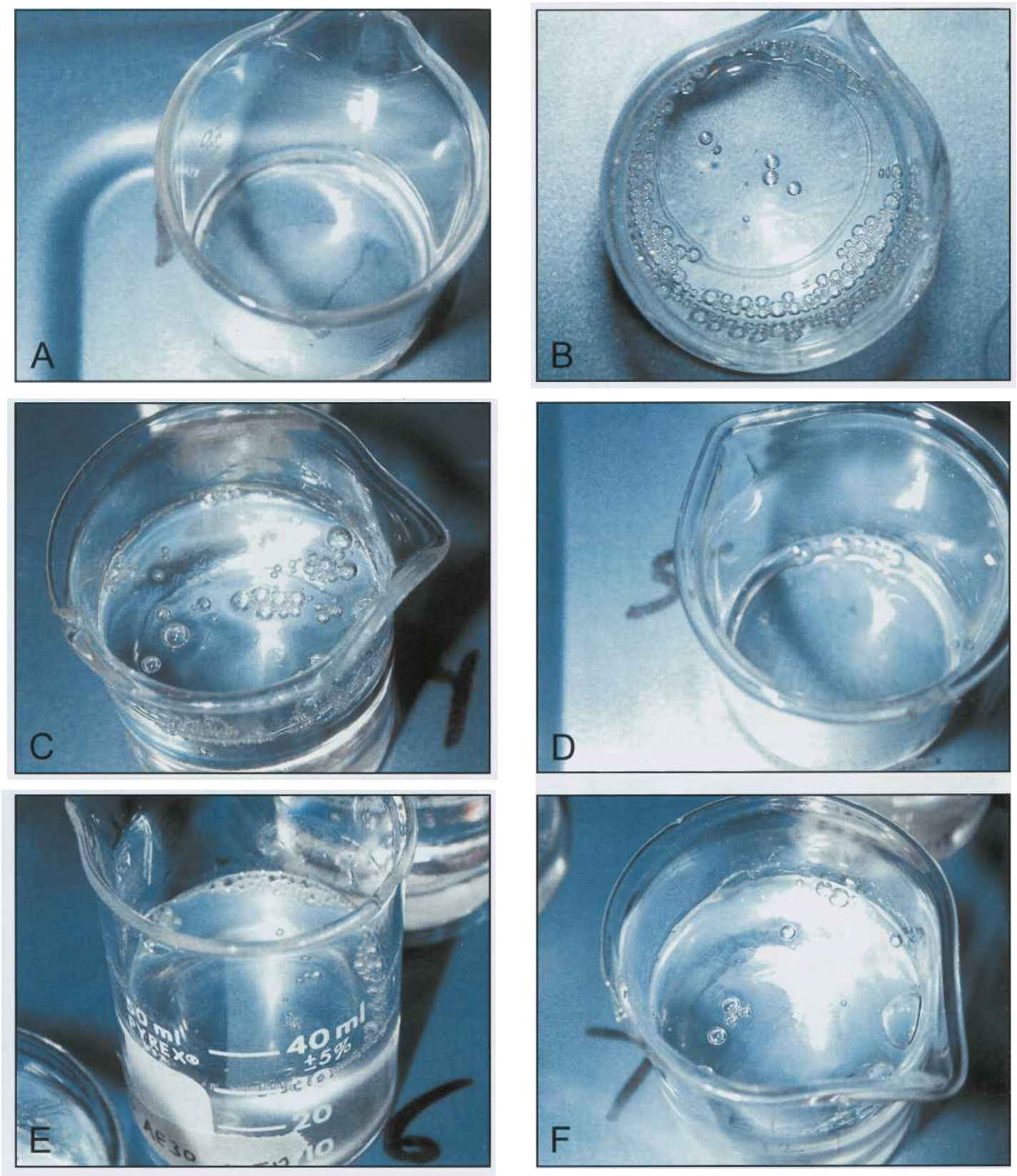

Figure 1. Components of epoxy reaction mixture at 10.3 cm of Hg. El hardener (A); E12 polymer (B); El and E12 (C); El and AE30 glass separator (D); E12 an AE30 (E); E1, E12 and AE30 (F).

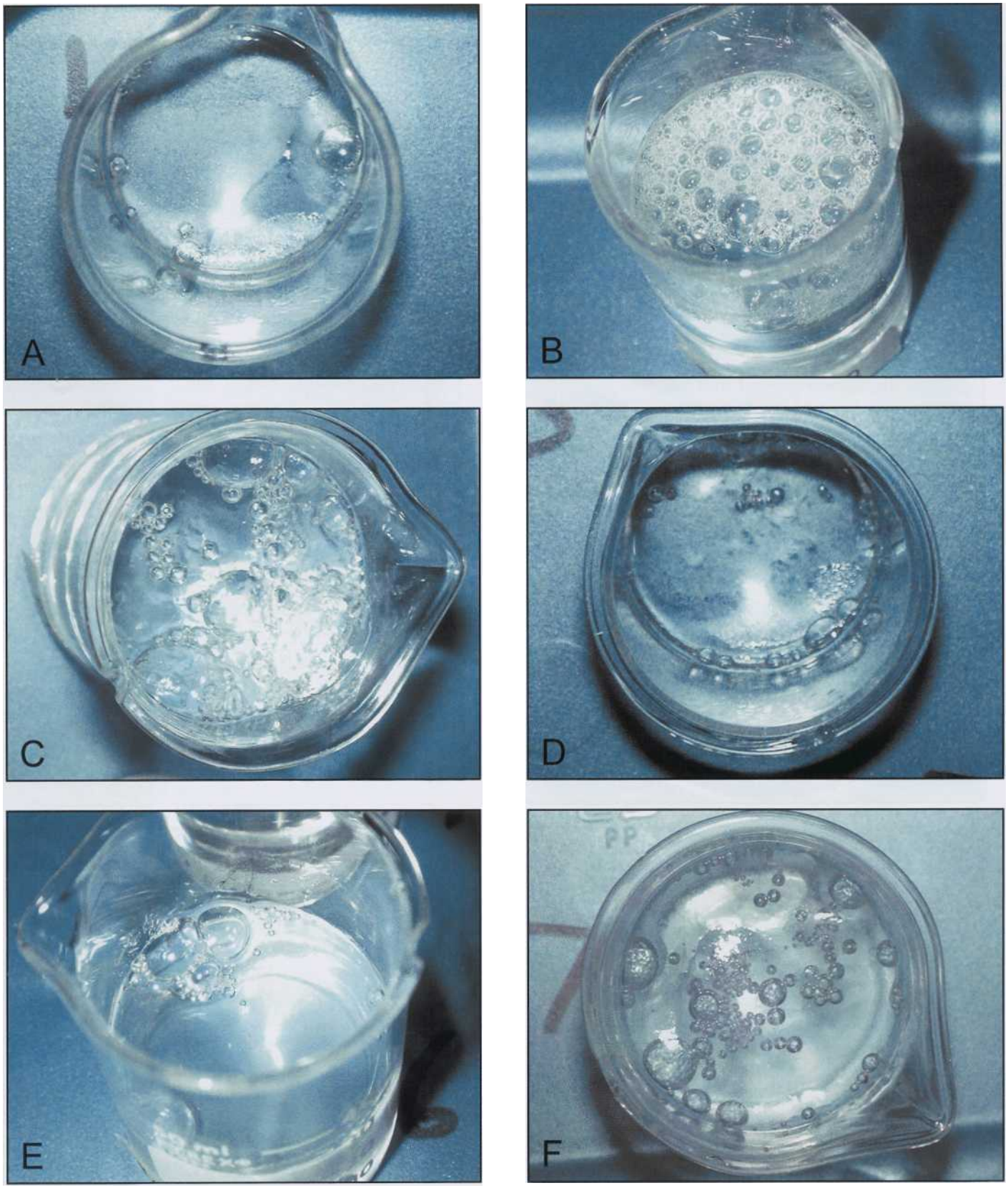

Figure 2. Components of epoxy reaction mixture at 1.0 cm of Hg. El hardener (A); El2 polymer (B); El and El 2 (C); El and AE30 glass separator (D); E12 an AE30 (E): El. E12 and AE30 (F).

had ceased. Beakers were then kept at room temperature (22-23°C) on a table where they were exposed to both natural and fluorescent light.

Forty-eight hours after the experiment began, the reaction mixtures containing the polymer + hardener and the polymer + hardener + glass separator had cured and were solid. The mixture with no separator cured crystal clear while that with the separator appeared turbid. The beakers with reaction mixtures containing the polymer + hardener and the polymer + hardener + glass separator which had cured contained air bubbles on the bottom of the beakers. Forty-eight hours after the experiment began, the beakers containing hardener alone and hardener + glass separator had sticky, semi-solids present in them. Forty-eight hours after the experiment began, the contents of the beakers containing polymer alone and polymer + glass separator remained in liquid form.

One month following completion of bubble production in the beakers, the contents did not differ from the way they appeared 48 hours post-experimentation with the exception of the beakers containing hardener and hardener plus separator showing a roughened surface to the semi-solid, sticky substance.

One hundred eighty days after the vacuum test, the contents of beakers #2 (El2) and #6 (El2, AE30) were still clear liquid. The contents of beakers # 1 (El) and #5 (El, AE30) were an opaque liquid with a thick film formed over the surface. The liquid in beaker #1 was almost gelatinous in consistency. The contents of beakers #4 (El, E12) and #7 (El, E12, AE30) were hardened and clear. The cured epoxy in beaker #4 was crystal clear while that in beaker #7 exhibited a slight opaqueness.

Discussion

Bubble production in the test beakers began at three different points during the experiment. The first bubbles generated in the beakers were most likely comprised of air which was dissolved in the reaction mixtures prior to their introduction into the vacuum chamber. These bubbles were not visible in the beginning of the experiment but were produced by a moderate decrease in pressure (12.5 to 15.0cm Hg gauge pressure). This initial bubble production occurred randomly across the samples with some of the beakers not showing any bubble production. This demonstrates that even moderately reducing pressure can produce more bubbles than were present before the vacuum was initiated and is apparently not linked to any one component of the reaction mixture. The fact that the beaker containing hardener with separator as well as the beaker containing all 3 components showed only very slight air bubble production when compared to the others might simply be due to a lower concentration of air in the mixtures when compared to the others prior to their placement into the vacuum chamber.

Subjecting epoxy reaction mixture to extreme reductions in pressure releases components of the mixture in a gaseous form into the casting chamber. A second wave of bubble production occurs when vacuum chamber pressure of less than 10.0cm Hg causes the release of a component of the El2 polymer in a gaseous form. A vacuum chamber pressure of less than 1.0cm Hg causes release of a gaseous component of the El hardener in a third wave of bubble production. One can be fairly certain that these gas bubbles are being released from the chemicals present in the reaction components as they were specific to the contents of the beakers as well as to two different pressure measurements. All beakers containing El2 began to show bubble production once the manometer reached 10.0cm Hg. The beakers containing El, which were not previously bubbling due to any El2 present in them as well, began to bubble at 1.0cm Hg. This shows a clear correlation between pressure and bubble production by the two components of the reaction mixture. Additionally, it is doubtful the bubbles produced after the pressure dropped to 10.3cm and lower were due to air because of the vast amount of bubbles generated.

Bubbles were not produced in the beaker containing the glass separator. Because this beaker was empty at the end of the experiment, it is obvious that the compound simply vaporized from the surface of the liquid without bubble production. The few bubbles produced at 10.3cm of Hg in the beaker containing the hardener plus glass separator were most likely glass separator bubbling up through the hardener. This can be assumed because the beaker containing only hardener produced no bubbles at the same reduction in pressure.

Release of these gas bubbles from El and E12 apparently does not affect their ability to fully cure when both are present in the same mixture. This might suggest that it is not just a portion of these chemicals which is being released but the actual vaporization of the entire compound. However, when bubble production ceased, the beakers containing El alone and El2 alone still contained liquids. Thus, vaporization of the entire product can be ruled out as the source of the second and third appearances of bubbles.

The release of these components of El and El2 produces an increase in the amount of bubbles present in the reaction mixture and decreases the aesthetics of the finished product. This is counterproductive to the employment of a vacuum chamber to remove air

bubbles from the casting chambers during epoxy plastination of tissues. Thus, placing epoxy reaction mixture under vacuum to aid in air bubble removal when plastinating at room temperature should be done at less than 12.5cm Hg gauge pressure so as not to produce more bubbles than were initially present. Filling casting chambers carefully to avoid introduction of air bubbles and teasing out the bubbles which inevitably become trapped is most likely the safest approach in reducing air bubble artifacts in epoxy slices.

Adding glass separator to the reaction mixture may be responsible for the turbid streaking seen in the clear areas of some epoxy plastination slices. Further studies must be conducted to determine this definitively. The roughened surface observed on the contents of the beakers containing hardener and hardener plus the glass separator 48 hours after experiment completion was most likely due to desiccation of the semi-solid contents.

Literature cited

Cook P. 1997a: Sheet plastination as a clinically based teaching aid at the University of Aukland. Acta Anat 158(l):33-36.

Cook P. 1997b: Submacroscopic interpretation of human sectional anatomy using plastinated El2 sections. J Int Soc Plastination 12(2): 17-27.

Guhr A, Mueller A, Anton H, von Hagens G. 1987: Complete examination of mastectomy specimens using sheet plastination with epoxy resin. J Int Soc Plastination l(l):23-29. Henry R.W., Thompson J.R.: Vacuum, vacuum gauges and monometers. J Int Soc Plastination 6(1): 10.

Latorre RM, Reed RB, Gil F, Lopez-Albors O, Ayala MD, Martinez-Gomariz F, Henry RW. 2002: Epoxy impregnation without hardener: to decrease yellowing, to delay casting and to aid bubble removal. J Int Soc Plastination 17:17-22. Mathura G. 1996: Problem encountered in El2 sheet plastination technique. J Int Soc Plastination 11:13.

Phillips MN, Nash LG, Barnett R, Nicholson H, Zhang M. 2002: The use of confocal microscopy for the examination of El2 sheet plastinated human tissue. J Int Soc Plastination 17:12-16. Skalkos E, Williams G, Baptista CAC. 1999: The E12 technique as an accessory tool for the study of myocardial fiber structure analysis in MRI. J Int Soc Plastination 14(1): 18-21. von Hagens G. 1985: Heidelberg Plastination Folder: Collection of all technical leaflets for plastination. D-6900 Heidelberg, Germany: Anatomisches Institut I, Universitat Heidelberg, von Hagens G. 1989: Biodur™ Products: Polymers, auxiliaries and equipment for plastination. A catalog and price list. Rathausstrasse 18, Heidelberg, Germany: Biodur, p. 34-35. Weber W, Henry RW. 1993: Sheet plastination of body slices - El2 technique, filling method. J Int Soc Plastination 7:16-22.

Journal of the International Society for Plastination 18:9-13 (2003)

Enhancing the Value of Organ Silicone Casts in Human Gross Anatomy Education

A. AULTMAN, J. BLYTHE, H. SOWDER, R. TROTTER and A. RAOOF*

Division of Anatomical Sciences, Office of Medical Education, The University of Michigan Medical School, Ann Arbor, Michigan, 48109-0608, USA.

Correspondence to: Office of Medical Education, The University of Michigan Medical School, 3808 Med. Sci. IIBldg., Ann Arbor, Ml, 48109-0608, USA; Telephone: 734-615 2597; Fax: 734-615 8191; E-mail: ameedr@umich.edu

Abstract: Medical students studying human gross anatomy often have difficulty conceptualizing the internal three-dimensional structure of organs and the pattern of distribution of blood vessels. Students are further challenged with comprehending the orientation and spatial relationship different organs have to one another as they function as integral parts of systems. Although tracheobronchial and heart casts of animals have been produced and have proven to be valuable tools in veterinary medical education (Henry, et al., 1992, 1998), few efforts have been made to develop physical models of these internal structures in humans for use in medical education. In this work, colored silicone casts of a human heart, tracheobronchial tree, and brain ventricles were made from unembalmed organs. Major vessels were cannulated and appropriately colored silicone was injected. Specimens were macerated to yield resilient, anatomically exact replica of the internal architecture such as cardiac chambers, lung vessels and airways, and the brain ventricular system.

*Key **words:*** **cast; silicone; tracheobronchial; ventricles**

Introduction

Research has indicated that engaging multiple senses enhances learning in academic settings. (Kundall, 1990; Westman, 1990). One of the challenges facing medical educators is presenting the circulatory and respiratory systems of humans, namely the heart and the lungs; in such a way that conceptualization of their spatial interaction and interdependence is achieved. Visualizing pulmonary and systemic circulations through the chambers and great vessels of the heart and the pulmonary vessels of the lungs, and relating these to the tracheobronchial tree, is difficult for medical students to understand using two-dimensional illustrations, dissections, videos and computer simulations.

Color-coded casts of the heart/lung system have proven invaluable for teaching medical gross anatomy. By acquiring greater understanding of the spatial relationship of overlapping circulatory vessels and the lobes of the lungs, for instance, students are better equipped to efficiently and accurately examine patients and to interpret diagnostic images of the thoracic cavity. The anatomical accuracy and durability of casts make them powerful tools to accelerate knowledge acquisition and strengthens diagnostic abilities for medical students utilizing a wider variety of learning strategies.

Materials and methods

The tracheobronchial, heart, and brain casting techniques used in this work were based on those of Tompsett (1970); Henry et al. (1992, 1998); and Grondin et al. (2000).

Preparation:

The heart, lungs, and brain were freshly harvested from human cadavers donated to the University of Michigan Anatomical Donation Program. Initially, all vessels and passageways of each organ were thoroughly rinsed with warm water to remove residual blood clots. Specimens were placed in a running water bath overnight before injection commenced the following day. If injection was planned for a later time, 3-5% formaldehyde was added. Water remaining in the vessels was flushed out using compressed air before injection.

Brain specimens were kept in 5% formaldehyde solution for about 3-5 days to ensure sufficient firmness during handling.

Three lungs and 2 heart-lung specimens as well as two brains were used in this work. All rubber cannulas used for injecting silicone were made of clear vinyl tubing of _ inch inner diameter fitted with a steel screw-type syringe adapter on one end.

Heart-lung specimen: Both lungs and heart were kept connected to each other. The pericardium was removed and the inferior vena cava was clamped with a hemostat. A 15 inch long cannula was pushed into the superior vena cava, through the tricuspid valve to the right ventricle, and into the pulmonary conus. A short incision, approximately an inch in length, was made in the ascending aorta and a second similar cannula was inserted into the left ventricle and then pushed through the mitral valve into the left atrium. This procedure ensured that the silicone would fill up the pulmonary veins. Cannulas were firmly retained in place with a piece of waxed string.

Lung specimen: The pulmonary artery and vein were cannulated. A third cannula was inserted and bound in the trachea for subsequent injection of the airways of the lungs. Cannulas used here were 10 inches in length. (Fig. 1).

Brain: A one inch diameter opening was drilled at the top of each cerebral hemisphere at the site of the central sulcus using an ordinary brass cork borer to provide access to the lateral ventricles. The ventricles were flushed with water and a 6 inch cannula was gently inserted into one opening (Fig. 2).

Silicone injection:

The specimens were injected with E RTV Silicone (Dow Corning, Midland, MI, USA) at room temperature. The silicone was colored red and blue with Biodur E20 (Biodur, Heidelberg, Germany) until the desired color shade was achieved. RTV Silicone Rubber Curing Agent was added at a 1:10 ratio to the silicone polymer immediately prior to injection. Injection was achieved using 60ml syringes filled with 35ml aliquots. The viscosity of the silicone was high enough to necessitate the use of a caulk gun to force the compound through the syringe into the cannula. Filling the syringe to 35ml extended the length of the syringe so that it was able to fit into the caulk gun. In the lungs, injection was stopped when silicone was visible under the surface of both lungs. In the heart-lung specimen, cannulas were pulled out slowly and gradually while injection was still maintained to ensure that silicone would fill the atria and ventricles. Silicone was kept from oozing out by using hemostats and waxed strings whenever necessary.

In the brain, silicone was gently pushed into one cannula and injection was stopped when silicone started emerging through the opening on the next hemisphere.

Curing:

Following injection, the silicone was allowed 24-48 hours at room temperature to harden before maceration.

Maceration:

After the silicone hardened, specimens were placed in a freshly prepared 10% potassium hydroxide (Potassium Hydroxide Flakes, Fisher scientific, USA) solution for 5-7 days and then left in boiling water for 8-12 hours to detach tissues from the polymer. Following maceration in boiling water, the specimens were placed in 5% hydrogen peroxide for about 2 hours to complete the removal of residual tissues. Casts were then rinsed in running water overnight.

Results

Casts of tracheobronchial tree, heart chambers, and brain ventricles were of excellent quality in terms of flexibility, clarity of details, and anatomical accuracy. The tracheobronchial and vascular tree casts showed clear color distinction that was clear throughout the minor bronchioles and vascular branching (Figs. 3, 4). Brain ventricular casts showed lateral ventricles, the third and most of the fourth ventricles with almost complete filling (Fig. 5).

Silicone injection through vessels was relatively effortless when the concentration of formaldehyde during preparation stage was 5% or less. Higher concentrations of formaldehyde made vessels firmer and hence injection was difficult. Also, we found that the degree of silicone flow through vessels and ventricles as well as the time needed for complete hardening following the injection were directly related to the concentration of the RTV Silicone Rubber Curing agent where 10% gave optimal results. Regarding maceration, better results were produced using fresh

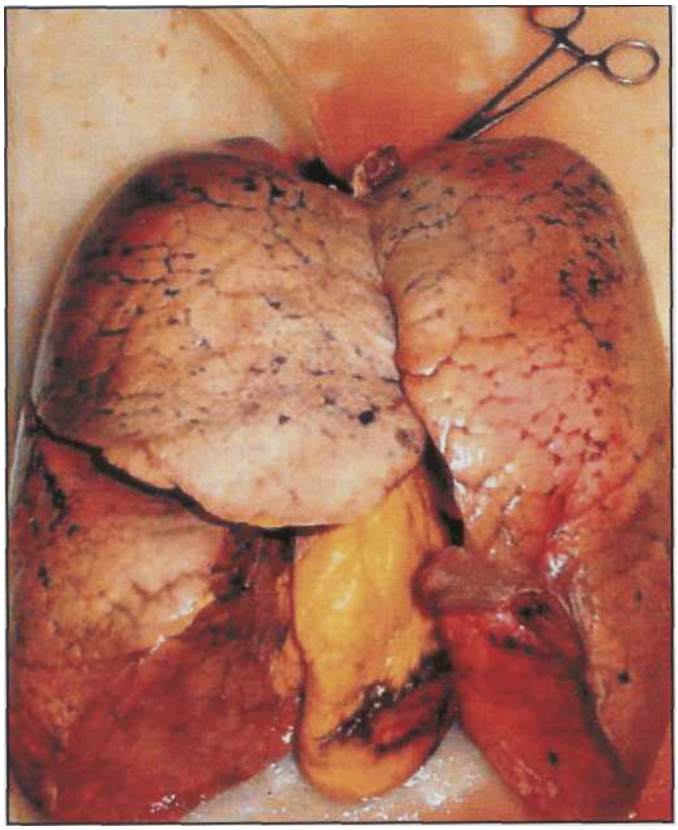

Figure 1. Preparation of a lung-heart specimen for silicone injection.

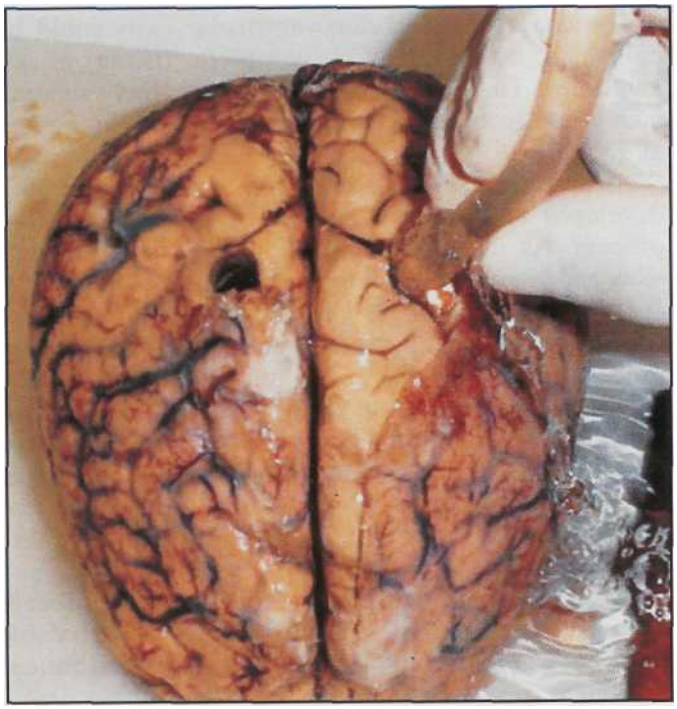

Figure 2. Cannulation of brain specimen before injecting silicone.

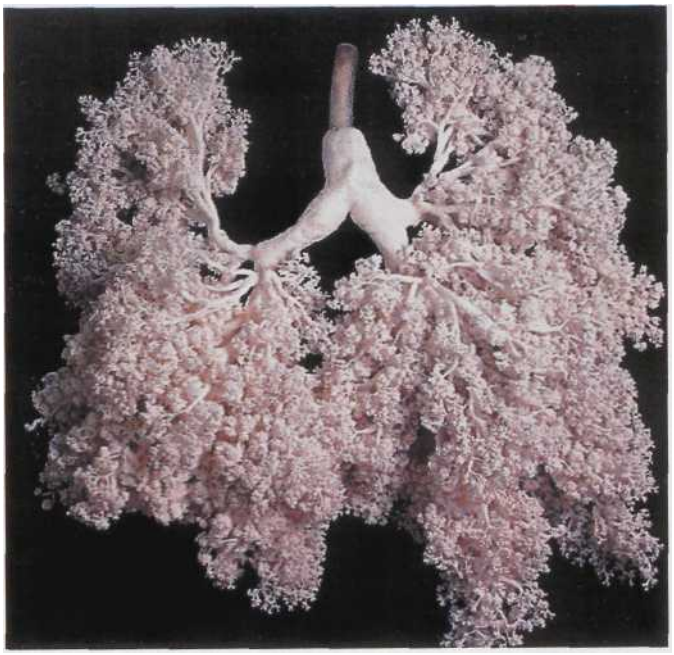

Figure 3. Tracheobronchial silicone cast.

Figure 4. Tracheobronchial and heart cast using colored silicone.

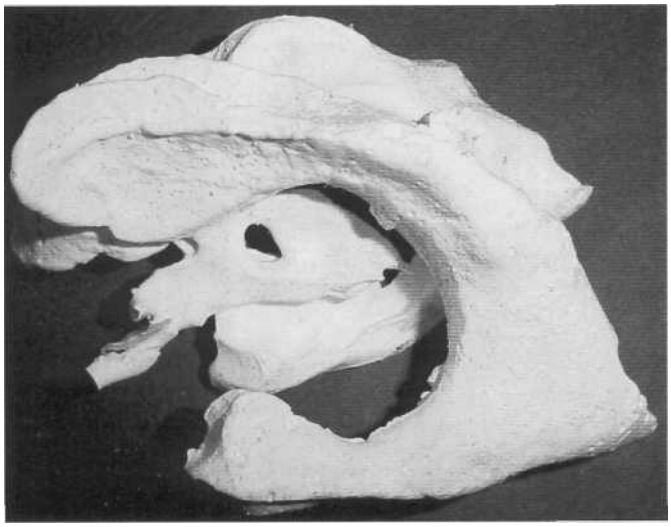

Figure 5. Brain ventricular cast.

10% potassium hydroxide for 5-7 days followed by boiling. Higher concentrations of potassium hydroxide or longer immersion of organs resulted in digestion of the silicone casts and loss of vascular fine details.

Discussion

Silicone casts of vessels, tracheobronchial tree, and brain produced in our lab were sturdy and anatomically precise. Specimens' sturdiness was generally assessed in terms of flexibility during regular handling and stretching. Used to enhance medical student learning in gross anatomy, these casts provide precise visual representations of the difficult to perceive internal architecture of these organs. Consequently, knowledge acquisition by students may occur faster as they employ multiple senses to both see and feel actual representations of each organ. Coupled with the use of silicone-plastinated hearts and lungs conceptualization of difficult physiological processes within these organs is made easier. Students' knowledge, clinical examination and diagnostic skills, accordingly, are enriched. During gross anatomy lab sessions at our medical school, medical students attended the course often used these casts in understanding the complex patterns of the tracheobronchial tree and the brain ventricular system. A formal study based on a thorough questionnaire to assess the usefulness of these casts in medical education is under preparation.

Some challenges for production of silicone casts of specimens arising from human cadavers, however, should be noted. At the University of Michigan, over 90% of anatomical donations are from elderly patients. Hence, a variety of clinical conditions may be encountered that impede quick and efficient production of silicone casts. In one specific case, a donor whose heart and lungs were slated for casting suffered a cardiac tamponade resulting from a ruptured aorta. Though the ruptured aorta was surely the cause of death, apparent pneumonia developed in the right lung before death and severely diminished the integrity of the lung. As a result, the lung was rendered useless for casting purposes due to deterioration of most of the tracheobronchial pathways. Some damage also occurred to the lung tissue during harvesting due to extensive adhesions to the thoracic wall.

In another incident, red-colored silicone injected into the pulmonary vein in an attempt to fill the left atrium and ventricle of another donor, had filled the entire heart instead. One possibility for this occurrence was that the donor suffered from a congenital septal defect that became apparent during the casting process.

Collapsed lungs, breast cancer metastasis into internal organs, and excessive accumulations of fat in and around organs of interest are further medical phenomena that can encumber the casting process. While human anatomical donations given to further the pursuit of medical knowledge, full-scale production of accurate, detailed casts must respectfully yield to the weakened state of some donors' organs, many which arise from older individuals. However, castings of pathological specimens may in time provide a valuable tool of comparison between normal and pathological specimens. Also, we are working on casting other organs like the liver and vascular casts of brain and kidneys.

The quality of the brain ventricular casts could be enhanced by ensuring a complete filling of all ventricles. This issue is currently under investigation taking into account the technique applied by Grondin et al. (2000).

An air pressurized injection method is being developed to add speed and efficiency to the casting process. As it is, the injection process is sometimes slow and laborious. With the increasing demand for the specimens and number of students handling these specimens, there is a need to accelerate the injection process. The air-pressurized method, utilizing the compressed air available at the lab, will allow us to quickly inject a number of specimens. It will also allow a more controlled flow of silicone with the use of pressure gauges and shut-off valves. With these two factors, we plan to create a plentiful stock of higher quality casts.

It is hoped that organ casting will make a significant contribution to medical education being an affordable and easy technique for visualizing anatomical specimens.

Literature cited

Grondin, J., Sianothai, A., Olry, R. 2000: In situ ventricular casts of S10 plastinated human brains. J Int Soc Plastination 15(1):18-21.

Henry RW, Daniel, GB, Reed, RB. 1998: Silicone Castings of the Chambers of the Heart and the Great Vessels. J Int Soc Plastination 13(1):17-19.

Henry, RW. 1998: Silicone Tracheobronchial Casts. J Int Soc Plastination 6:38-40.

Kundel, HL. 1990: Visual clues in the Interpretation of Medical Images. J Clin Neurophysiology 7(4):472-83. Westman, AS. 1990: Picture books, not readers!

Teachers use the wrong modality in presentations and students in studying. Percept Mot Skills 70(3, part 1): 840-2. Oleksik, SA. 1987: Learning through Visualization.

Nurse Educator 12(6):36-7. Tompsett, D.H. 1970: Anatomical Techniques. Second

edition, E. & S. Livingstone, London.

Journal **of the International Society for Plastination 18:14-22 (2003)**

P-40 and S10 Plastinated Slices: An Aid to Interpreting MR Images of the Equine Tarsus

R. LATORRE[1]*, A. ARENCIBIA[2], F. GIL[1], M. RIVERO[2], G. RAMIREZ[1], J.M. VAQUEZ-AUTON[1] and R.W. HENRY[3]

'Anatomia y Embriologia, Facultad de Veterinaria, Universidad de Murcia, Campus de Espinardo, 30071, Murcia, Spain. [2]Departamento de Morfologia, Facultad de Veterinaria, Universidad de Las Palmas de Gran Canada, Trasmontana, 35416, Arucas, Spain. ^Department of Comparative Medicine, College of Veterinary Medicine, University of Tennessee, 2407 River Drive, Knoxville, TN, 37996, USA.

Correspondence to: Telephone: 34 - 968 - 364 - 697; *Fax:* 34 - 968 - 364 - 147; *E-mail:* latorre@um.es

Abstract: The efficacy of a combined use of P-40 and S10 Biodur™ techniques as an aid for radiographic anatomy is investigated. The purpose of this study was to use a combination of P-40 and S10 plastinated slices and magnetic resonance (MR) images to better understand the anatomy of the normal adult equine tarsus. Tarsi from four normal pure breed Spanish horses were utilized. The sagittal and transverse MR images were performed using a scanner with a 1.5 Tesla magnet. Macroscopic slices (2mm and 10mm in thickness) that correlated with the MR images were obtained from distal limbs whose synovial space (tarsocrural joint) and blood vessels were injected with colored latex. The results demonstrate that a combined use of semitransparent slices (P-40) and thick (S10) slices from the imaged specimens allows an accurate evaluation in MR images of many anatomic structures.

Key words: **anatomy; equine; plastination; polymer; P-40; S10; tarsus**

Introduction

Imaging technologies such as magnetic resonance imaging (MRI), computed tomography (CT) and ultrasonography have created a need for in depth studies of sectional anatomy. Most of the combined anatomic and diagnostic explorations using MRI or CT used lcm thick macroscopic tissue sections which yielded good correlation of the tissue slices with the CT image (Denoix et al., 1993; Blaik et al., 2000; Vazquez et al., 2001). Classically these slices have been on fresh tissue that was later fixed. Unfortunately, body slices prepared by traditional formalin fixation methods are often unpleasant to handle and prone to deterioration. Various polymers such as silicone (Cooper et al., 1990; Weiglein, 1996), polymerizing emulsion (Margios et al., 1997), epoxy (von Hagens, 1979; Entius et al., 1993; Weber and Henry, 1993) and polyester (Weiglein et al., 1997; Sora et al., 1999) have been used for producing anatomical slices to be compared with radiographic material. Each polymer yields different results. Silicone impregnated specimens are opaque, somewhat flexible and resilient. Polymerizing emulsion has been used for the plastination of extremity or body slices, but this process yields firm, opaque slices (Marigos et al., 1997). Epoxy resins are used for study of sectional anatomy with thin semitransparent body slices (2mm thickness) (von Hagens et al., 1987;

Enitius, 1993; Cook, 1997). The common epoxy technique for over two decades has been El2 sheet plastination. Polyester resin has been routinely used only for brain slices, resulting in excellent distinction between gray and white matter (von Hagens et al., 1987).

The aim of this work was to demonstrate that: 1. The P-40 technique can also be used to preserve semitransparent body slices, and 2. A combined use of these two plastination methods (S10 and P-40) can aid in a more accurate interpretation of MR images, than using only one technique.

Materials and methods

Four Spanish pure breed horses were donated to the Large Animal Hospitals (Universities of Murcia and Las Palmas de Gran Canada. Spain). Their pelvic limbs were removed and used for this study and in conjunction with other research projects. These tarsi were scanned within 2 hours of euthanasia. At the conclusion of MR imaging, the arteries, veins and synovial spaces of the cleaned and shaved tarsi were injected with red, blue and green latex, respectively. To produce these colors, white latex was colored using pigment paste (2% ppv): AC50 (red), AC52 (blue) and AC54 (green) (Biodur™, Heidelberg). The femoral artery was used for arterial injection. Injection was concluded when latex oozed from the smaller cut arteries. Then one of the two plantar digital veins was used, as distal as possible, to inject the venous system. Proximally the veins were ligated when blue latex reached the open end. The plantar pouches (lateroplantar and medioplantar) were utilized for injection of the tarsocrural joint space. Sagittal and transverse slices were then prepared to demonstrate the anatomic relationships of structures of the tarsus.

MR Images

A Genesis-Sigma scanner (General Electric Medical Systems from Special Diagnostic Service of San Roque Clinic, Ayalon, Las Palmas de Gran Canaria, Spain) was used to produce MR images. The unit had a superconducting magnet operating at a field of 1.5 Tesla. To obtain the images, the specimens were placed, with the tarsal and digital joints in extension, within a human extremity coil. Images were acquired using a spin echo pulse sequence. Sagittal and transverse images were acquired in proton density (PD) weighted with the parameters show in table 1.

Two hundred and thirty MR images were taken at the various tarsal joint levels (transverse and sagittal). Images that had the best correlation with the sagittal and transverse macroscopic slices were selected.

	Sagittal	Transverse
Repetition time	3160 msec	3160 msec
Echo	14 msec	15 msec
Echo number	1	1
Number of excitations	1	1.5
Matrix size	512X224	512X224
Slice thickness	6mm	6mm
Spatial resolution	1 lmm	11mm

Table 1. Parameters of MR imaging equipment for acquiring PD-weighted sagittal and transverse images of the adult equine tarsus.

Slicing

After latex injection, the limbs were frozen at -80°C. After freezing, transverse and sagittal slices were made from the distal tibia to the proximal metatarsus on a high-speed band saw at desired thicknesses (2mm and 10mm). Liquid nitrogen was used to cool the saw table for production of the 2mm slices. The following slicing pattern (10mm/2mm/2mm/10mm/2mrn/2rnm/10mm) was used. Slices were placed on grids. Saw dust was removed by submerging tissue slices in cold acetone and scraping, or flowing a small stream of cool tap water quickly across the slice. A minimum of twenty slices were made from each tarsus. Both surfaces of each slice were photographed prior to fixation. Standard P-40 and S10 techniques (von Hagens, 1985; von Hagens et al., 1987; Henry and Nel 1993) respectively were used to plastinate the 2 and 10mm slices.

Fixation

Only the 10mm thick slices were fixed. These slices were submerged in a 10% formaldehyde solution for 15 days at cool temperature (2°C). After removal from the fixative, they were washed under running tap water for one day.

Dehydration

The slices were dehydrated in cold acetone (freeze substitution). Cleaned slices on their grids were submerged in vats containing 10X the specimen volume of 90% acetone at -20°C. Two changes of 100% cold acetone were carried out at weekly intervals.

Forced Impregnation

After dehydration, the slices were separated into two groups. Group 1 consisted of the 10mm thick tissue slices which were plastinated according to the standard cold S10 technique (Biodur™). Group 2 consisted of all the 2mm thick tissue slices which were plastinated at room temperature using the P-40 technique (Biodur™).

Reaction mixtures

Group 1: Polymer SR10 + Catalyst SH03 (1% ppv) (Biodur™, standard silicone procedure, at -20°C) (von Hagens, 1985).

Group 2: Polymer P-40 (BiodurTM, room temperature polyester procedure) was used in a darkened chamber.

Tissue slices were immersed in the reaction mixtures and placed into a vacuum chambers. Pressure was gradually decreased for both groups until a pressure of <5mm Hg (group 1) and 10mm Hg (group 2) was attained. These pressures were maintained until bubbling ceased.

Curing

Group 1: The slices were removed from the polymer reaction mixture. Excess polymer was drained and wiped from the slices. The silicone impregnated slices were placed in an airtight container with S6 crosslinker (SH06 Biodur™) (von Hagens, 1985). The S6 was vaporized ten minutes daily using an aquarium pump. The slices remained in this environment one week. During this period the slices were turned and wiped of excess polymer three to four times a day. Finally, the slices were placed in a plastic bag containing vaporized S6 for 2 months allowing complete curing of the slices.

Group 2: Each impregnated slice was removed from the impregnation bath and placed into casting chambers fashioned from two sheets of 3mm tempered glass, a silicone gasket and fold back clamps (Weber and Henry, 1993). The chambers were filled with fresh P-40, closed and sealed with . The slices were exposed for four hours to ultraviolet-A lights. The UV-A light was alternately turned on for 15 minutes intervals and off for 30 minutes to avoid excess heat build up during this curing phase. During curing, a ventilator was used to cool the chambers. When the curing was completed, the glass chambers were dismantled and the slices trimmed.

Results

In this study, the plastination of tissue slices of the tarsus was a valuable tool for interpretation of tarsal MR images. Each slice and MR image provided detailed information on the anatomy for the equine tarsus. Both sagittal and transverse MR images, as well as, plastinated slices yielded remarkable detail (Figs, la, 2a, 3a,4a). In fresh macroscopic slices (Figs, lb, 2b, 3b, 4b), S10 plastinated slices (Figs, lc, 2c, 3c, 4c) and P-40 plastinated slices (Figs. Id, 2d, 3d, 4d) distinction of individual structures and their anatomic relationships were easily noted and remarkably useful when viewing and comparing to one another.

Sagittal sections (Figs. 1, 2) in general yield a clear differentiation between the tarsocrural, intertarsal (talocalcaneal, calcaneoquartalis, talocalcaneocentralis, centrodistalis), and tarsometatarsal joints. The semi-transparent plastinated macroscopic slices (P-40) accurately show the different ligaments (tibiocalcaneal, talocentrodistometatarsal, long plantar, tibiotalar) and other structures such as the tarsal sinus and tarsal canal. While S10 sections exhibit an excellent contrast between adipose tissue, which appears white, other tissues such as the lateral and medial plantar nerves and muscle bundles were also easily identified.

Transverse sections compliment MR images (Figs. 3, 4), and tarsal structures like tendons, intertarsal joints and synovial pouches could be identified. Plastinated transverse sections yielded much information about the extent of joint capsule and the relationship with collateral ligaments and bones (talus and calcaneus). Transverse S10 plastinated slices (Fig. 3c) displayed a superb differentiation of the dorsomedial, lateroplantar and medioplantar synovial pouches, and the medial (Cunean) tendon of tibialis cranialis. These structures were not as distinct in the MRI and P-40 plastinated slices. However, transverse plastinated P-40 sections (Fig. 3d) showed a clear differentiation between the tibialis cranialis, peroneus tertius and long digital extensor muscles. These muscles were more difficult to differentiate in the MR images and S10 plastinated slices. The relationships of the lateral digital extensor and medial digital flexor tendons and their relation with the collateral ligaments were easily analyzed in the P-40 transverse sections. However, these relationships were more difficult to discern in MR images and S10 plastinated slices.

Discussion

The tarsal joint is an anatomically complex area and an understanding of this is a prerequisite for accurate diagnosis of injuries in this joint. The results of this work show that the combined use of semitransparent (P-40) and thick (S10) slices from the same specimen each offer detailed information which can be an aid for interpretation of MR images.

Our results demonstrated that images from fresh macroscopic slices, before they were plastinated, were also useful to determinate some anatomical structures. This was especially such when comparing these images with the plastinated slices. We could not find any author who reported using recorded images prior to plastination to interpret the plastinated specimen.

The quality of S10 and P-40 plastinated and fresh slices was excellent. Many structures (vessels, synovial membrane or synovial sheaths) were more readily identifiable when the plastinated slices were compared

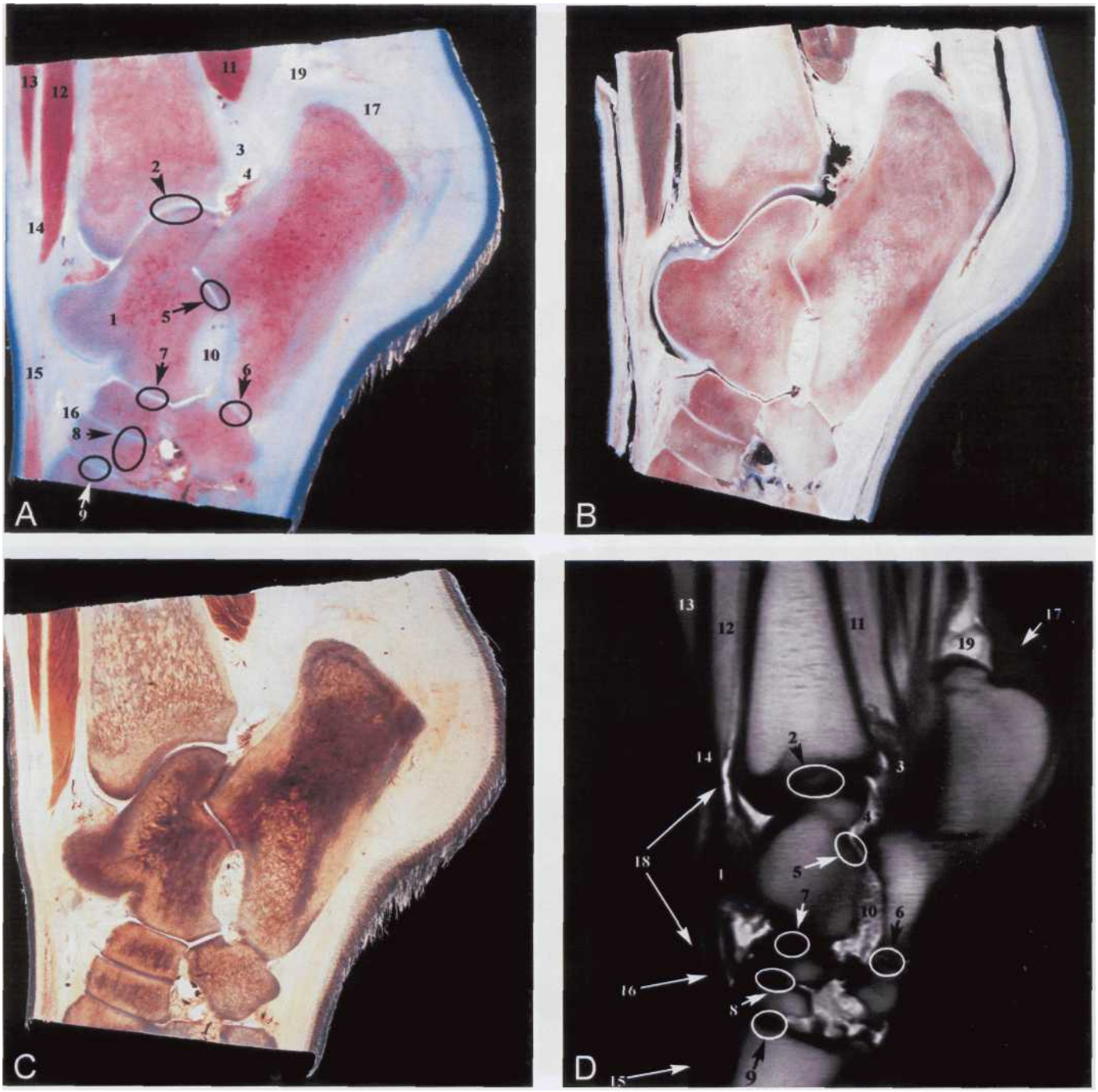

Figure 1. Sagittal sections of the equine tarsus: Fresh macroscopic section (A), S10 plastinated section (B), P-40 plastinated section (C), MR image (D). 1. Labium mediale trochlea tali, 2. Articulatio tarsocruralis, 3. Capsula articularis, 4. Recessus lateroplantaris (articulatio tarsocruralis), 5. Articulatio talocalcanea, 6. Articulatio calcaneocuartalis, 7. Articulatio talocalcaneocentralis, 8. Articulatio centrodistalis, 9. Articulatio tarsometatarseae, 10. Sinus tarsi, 11. M. flexor digitorum profundus, 12. M. tibialis cranialis, 13. M. extensor digitorum longus, 14. M. peroneus tertius, 15. M. extensor digitorum longus (tendo), 16. M. tibialis cranialis (tendo cranialis), 17. M. flexor digitorum superficialis (tendo), 18. Vagina tendinis (m. tibialis cranialis), 19. Bursa calcanea (m. flexoris digitorum superficialis).

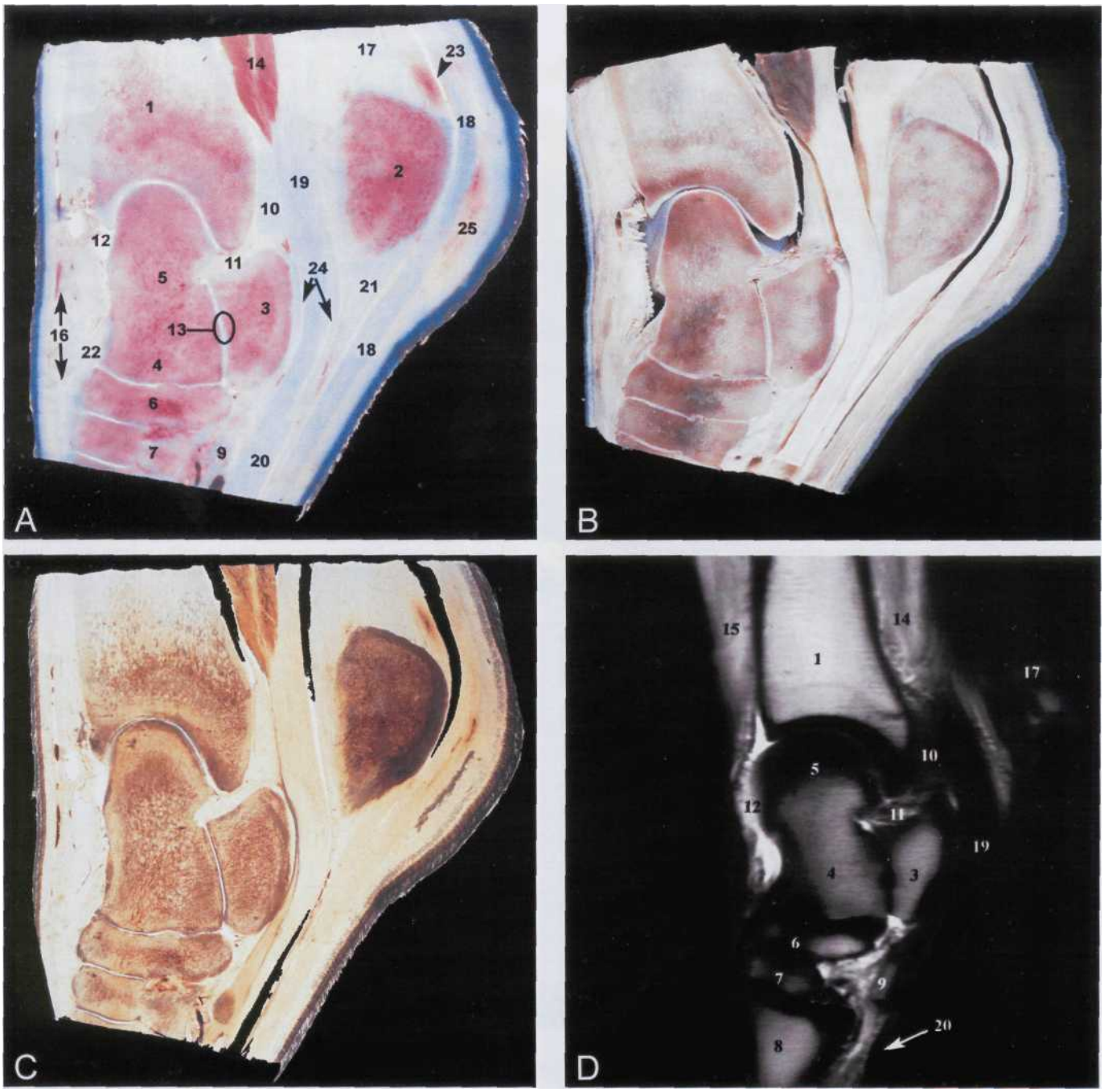

Figure 2. Medial parasagittal sections of the equine tarsus: Fresh macroscopic section (A), S10 plastinated section (B), P-40 plastinated section (C), MR image (D). 1. Tibia, 2. Tuber calcanei, 3. Sustentaculum tali, 4. Corpus tali, 5. Trochlea tali, 6. Os tarsi centralis, 7. Os tarsale III, 8. Os metatarsal III, 9. Os tarsale I + II, 10. Capsula articularis, 11. Ligamentum tibiocalcaneo plantaris, 12. Recessus dorsomedialis (articulatio tarsocruralis), 13. Articulatio talocalcanea, 14. M. flexor digitorum profundus, 15. M. tibialis cranialis, 16. M. tibialis cranialis (tendo medialis/cuneans), 17. Tendo calcaneus communis, 18. M. flexor digitorum supfercialis (tendo), 19. M. flexor digitorum lateralis (tendo), 20. M. flexor digitorum profundus (tendo), 21. Ligamentum plantare longum, 22. Ligamentum talocentrodistometatarseum, 23. Bursa calcanea m. flexoris digitorum superficialis, 24. Vagina tendinis m. flexor digitorum lateralis, 25. Bursa subcutanea calcanea.

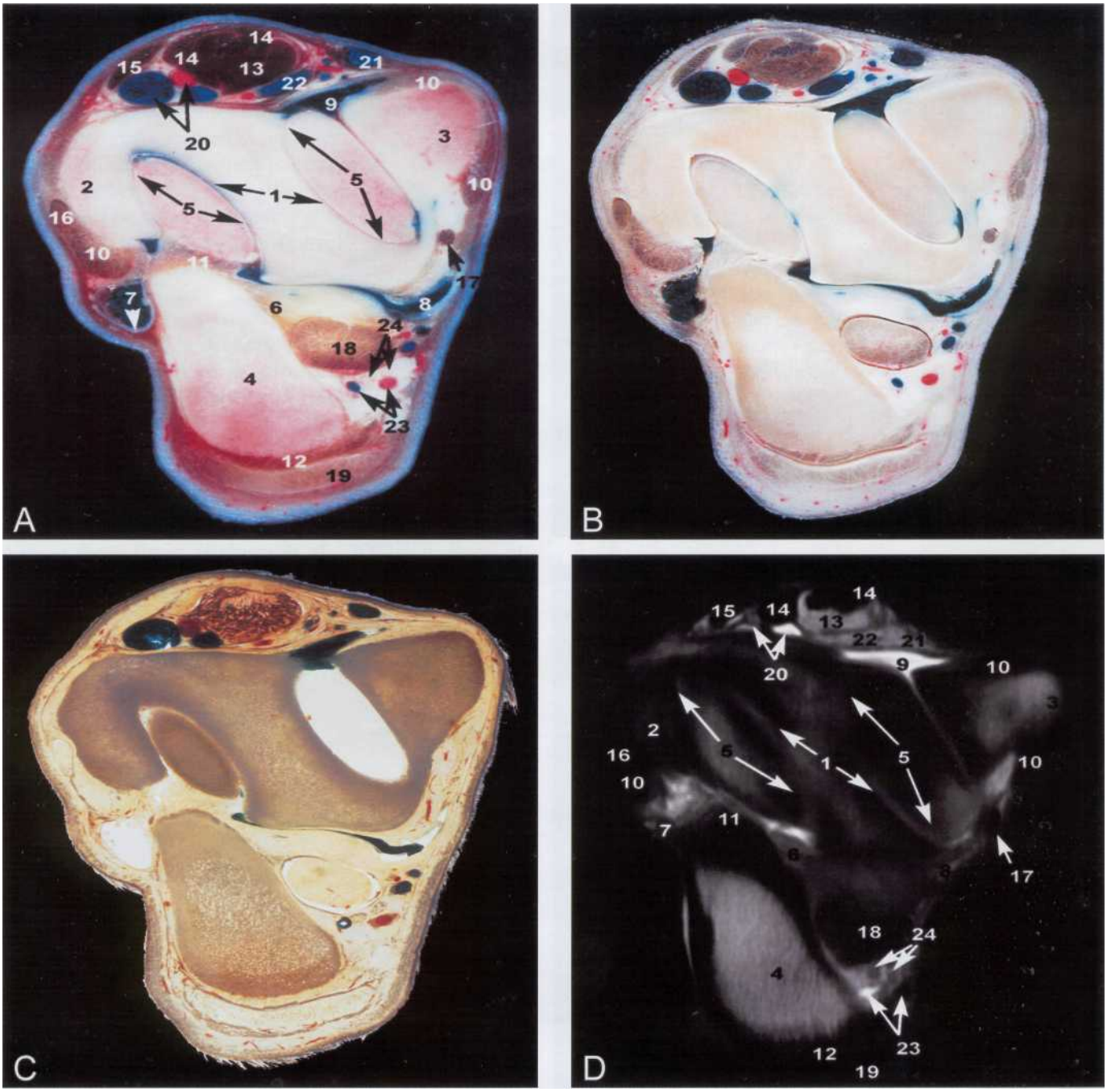

Figure 3. Transverse sections of equine tarsocrural joint: Fresh macroscopic section (A), S10 plastinated section (B), P-40 plastinated section (C), MR image (D). 1. Tibia (cochlea), cartilago articularis (arrow), 2. Malleolus lateralis, 3. Malleolus medialis, 4. Tuber calcanei, 5. Trochlea tali (labiae), cartilago articularis (arrow), 6. Capsula articularis, 7. Recessus lateroplantaris (articulatio tarsocruralis) (arrow), 8. Recessus medioplantaris (articulatio tarsocruralis), 9. Recesus dorsomedialis (articulatio tarsocruralis), 10. Ligamenta collateralia lateral et medial, 11. Ligamentum talocalcaneum laterale, 12. Ligamentum plantare longum, 13. M. tibialis cranialis, 14. M. peroneus tertius (tendo), 15. M. extensor digitorum longus (tendo), 16. M. extensor digitorum lateralis (tendo), 17. M. flexor digitorum medialis (tendo), 18. M. flexor digitorum lateralis (tendo) et m. tibialis caudalis (tendo), 19. M. flexor digitorum superficialis (tendo), 20. A. et v. dorsalis pedis, 21. V. saphena medialis (rama cranealis), 22. Anastomosis between v. saphena medialis and v. dorsalis pedis, 23. A. saphena (rama caudalis) et v. saphena medialis (rama caudalis), 24. Nn. plantaris lateralis et plantaris medialis.

Figure 4. Transverse sections of equine limb at the level of the central tarsal bone: Fresh macroscopic section (A), S10 plastinated section (B), P-40 plastinated section (C), MR image (D). 1. Os tarsi centralis, 2. Os tarsale IV, 3. Os tarsale I+II, 4. Canalis tarsi, 5. Articulatio centrodistalis, 6. Ligamenta collateralia tarsi laterale et mediale longum, 7. Ligamentum plantare longum, 8. Ligamentum talocentrodistometatarseum, 9. M. tibialis cranialis (tendo medialis/cuneans), 10. M. tibialis cranialis (tendo cranealis), 11. M. peroneus tertius (tendo cranealis), 12. M. extensor digitorum longus (tendo), surrounded by its vagina tendinis, 13. M. extensor digitorum lateralis (tendo), 14. M. extensor digitorum brevis, 15. M. flexor digitorum medialis (tendo), 16. M. flexor digitorum lateralis (tendo) et m. tibialis caudalis (tendo), 17. M. flexor digitorum superficialis (tendo), 18. A. et v. dorsalis pedis detaching the a. et v. tarsea perforans, 19. V. tarsea perforans occupying the canalis tarsi, 20. Aa et vv. plantares lateralis et medialis, 21. Nn. plantaris lateralis et plantaris medialis.

with their own fresh images. The shrinkage of surrounding connective tissue in S10 sections permits better identification of nerves. The better optical properties of some anatomic structures as ligaments and tendons in the P40 sections makes identification easier.

S10 plastinated sections provided confirmation that the MR images obtained were a true representation of that area of the body, which is consistent with previous reports (Cooper et al., 1990; Weiglein, 1996, Marigos et al., 1997). The direct comparison between sheet serial sections (P-40) and the equivalent MR images provided a clearer understanding of anatomical structures. This should enhance clinical interpretation and is similar to reports for E-12 sheet slices (Entius et al., 1993). The classic epoxy (E-12, Biodur™) method has been used for over two decades to produce routine slices in veterinary anatomy (Weber and Henry, 1993) or human anatomy (Entius et al., 1993; Cook, 1997). But epoxy often yellows within a few days or weeks after casting and when impregnation is complete there is only a short window of time in which to cast the slices (von Hagens, 1985). In this sense, several authors have worked to improve these limits (Latorre et al., 2002a, b; Reed et al., 2002). However, the results of P-40 sections in this study did not have these limitations. Our results with P40 were similar to those previously reported using polyester (P-35 or P-40) to preserve sheet body slices (de Boer-van Huizen et al., 1993; Latorre et al., 2002c; Weiglein et al., 2002).

The findings of this study indicate that the P-40 method (Biodur™) could be used to produce body sections for comparison with MR images. A combined use of transparent (P-40) and thick (S10) slices from the same specimen allowed an accurate evaluation of many anatomic structures in the MR images.

Acknowledgements: This work was supported by Seneca Foundation, Comunidad Autonoma de la Region de Murcia (project number: PC/2/FS/99). The authors wish to thank Mr. Mariano Orenes and Ms. Helena Abell&n of Murcia University for their excellent technical expertise in preparing the material; personal from Special Diagnostic Service of San Roque Clinic, Ayalon, Las Palmas de Gran Canaria, Spain, for their technological skills, time and patience throughout the MR scanning process.

Literature cited

Blaik MA, Hanson RR, Kincaid SA, Hatchcok JT, Hudson J A, Baird D K. 2000: Low-Field magnetic resonance imaging of the equine tarsus: normal anatomy. Vet Radiol & Ultrasound 41:131-141.

Cook P. 1997: Sheet plastination as a clinically based teaching aid at the University of Auckland. Acta Anat 158:33-36.

Cooper M. 1990: The technique and use of plastinated specimens in teaching and research: Gross anatomical sections of the head and neck. J Int Soc Plastination 4(1):4.

de Boer-van Huizen, RT, Cornelissen CJ, ten Donkelaar HJ. 1993: The P35 technique for sheet plastination of the human head. J Int Soc Plastination 7:36.

Denoix J M , Crevier N , Roger B, Lebas J F. 1993: Magnetic resonance imaging of the equine foot. Vet Radiol & Ultrasound 34:405-411.

Entius CAC, Kuiper JW, Koops W, de Gast A. 1993: A new positioning technique for comparing sectional anatomy of the shoulder with sectional diagnostic modalities: Magnetic Resonance Imaging (MRI), Computed Tomography (CT) and Ultrasound (US). J Int Plastination 7:23-26.

Henry RW, Nel PPC. 1993: Forced impregnation for the standard S10 method. J Int Soc Plastination 7:27-31.

Latorre RM, Reed RB, Gil F, Lopez-Albors O, Ayala MD, Martinez-Gomariz F, Henry RW. 2002: Epoxy impregnation without hardener: to decrease yellowing, to delay casting and to aid bubble removal. J Int Soc Plastination 17:17-22.

Latorre R, Vazquez JM, Gil F, Ramirez G, Lopez-Albors O, Ayala M, Arencibia A. 2002b: Anatomy of the equine tarsus: A study by MRI and macroscopic plastinated sections (S10 and P40). J Int Soc Plastination 17:6-7.

Latorre RM, Reed RB, Henry RW. 2002c: Epoxy impregnation with no hardener. J Int Soc Plastination 17:7.

Margios M, Kekic M, Doranet GA. 1997: Learning relational anatomy by correlating thin plastinated sections and magnetic resonance images: Preparation of specimens. Acta Anat 158:37-43.

Reed RB, Henry RW. 2002: Epoxy under vacuum. J Int Soc Plastination 17:8.

Sora MC, Brugger P, Traxler H. 1999: P40 plastination of human brain slices: Comparison between different immersion and impregnation conditions. J Int Soc Plastination 14(l):22-24.

Vazquez, JM, Rivero M, Gil F, Ramirez JA, Ramirez G, Vilar JM, Arencibia A. 2001: Magnetic resonance imaging of two normal equine brains and their associated structures. Vet Rec 148:229-232.

von Hagens, G. 1979: Impregnation of soft biological specimens with thermosetting resins and elastomers. Anat Rec 194(2):247-255.

von Hagens G. 1985: Heidelberg Plastination Folder: Collection of all technical leaflets for plastination. Heidelberg, Germany: Anatomisches Institut 1, Universitat Heidelberg, von Hagens G, Tiedemann K, Kriz W. 1987: The current potential of plastination. Anat Embryol 175(4):411-421. Weber W, Henry R W. 1993: Sheet plastination of body slices-El2 technique, filling method. J Int Soc Plastination 7:16-22. Weiglein AH, Henry RW. 1993: Curing (hardening, polymerization) of the polymer - Biodur S10. J Int Soc Plastination 7:32-35. Weiglein AH. 1996: Preparing and using S10 and P-35 brain slices. J Int Soc Plastination 10:22-25. Weiglein AH, Bahadori K, Feigl G. 1997: Congruent CT-scans and plastinated slices. J Int Soc Plastination 12(2):35. Weiglein AH, Kqiku L, Pertl C. 2002: Inferior alveolar nerve anatomy revisited: A study based on dissection and plastination. J Int Soc Plastination 17:10.

12 International Conference on Plastination
Murcia, Spain, July 11-16, 2004

Precongress workshop, July 10 and 11

Hosted by: Department Anatomia y Embryologia
Facultad de Veterinaria Universidad de Murcia

Contact: Dr. Rafael Latorre
e-mail: latorre@um.es
telephone: 34-968-364-697
fax: 34-968-364-147

Sponsored by: The International Society for Plastination

Journal of the International Society for Plastination 18:23-28 (2003)

Plastinated Ethmoidal Region: I. Preparation and Applications in Clinical Teaching

E. MUSUMECI[1], F.J.W. LANG[1], B. DUVOISIN[2] and B.M. RIEDERER[3]*

[1] *Service d'ORL et de Chirurgie Cervico-Faciale, CHUV, 1011 Lausanne, Switzerland.*
[2]*Service de Radiologic, CHUV, 1011 Lausanne, Switzerland.*
[3] *Inst it ut de Biologie Cellulaire et de Morphologie, Universite de Lausanne, Rue du Bugnon 9, 1005 Lausanne, Switzerland.*

**Correspondence to: Telephone:* 41-21-692 5154; *Fax:* 41-21-692 5105; *E-mail:* BeatMichel.Riederer@ibcm.unil.ch

Abstract: Ethmoidal regions were prepared and dissected to demonstrate regional sinus anatomy and endoscopic surgical approaches from six human heads. After preparation, the specimens were plastinated using the standard S10 technique. A CT-scan of each ethmoidal block was performed before and after preparation of the block to access shrinkage. The plastinated specimens were successfully introduced into clinical teaching of sinus anatomy and surgery. One advantage of using these specimens is their long-lasting preservation without deterioration of the tissue. The specimens are well suited for comparative radiographic and endoscopic studies, and the CT-scans allowed an exact measurement of tissue shrinkage due to plastination. Increased tissue rigidity and shrinkage due to plastination has to be taken into account for subsequent endoscopic observation.

*Key **words:*** **anatomy; computed tomography; endoscopy; plastination; radiology; sinus; surgery**

Introduction

In otorhinolaryngology endoscopic sinus surgery bears a potential danger of severe hemorrhage in the nasal, orbital and intracranial regions (Stankiewicz et al., 1987; Stammberger et al., 1990). To be able to perform such surgery, it is necessary for the surgeon to train on *ex vivo* ethmoidal blocks (EB), which have been previously removed from cadavers and dissected. However, it is increasingly difficult to obtain human bodies. For this reason, development of a reusable didactic tool that favors the study and the understanding of anatomical structures of the sinuses and the nasal cavity, as well as the study of the principles of basic surgical interventions is imperative. Plastination or polymer impregnation of tissue should render the ethmoidal blocks long lasting, without tissue decay. Furthermore, the use of plastinated EB should decrease the number of EB that have to be prepared for training programs each year. This report outlines a method of preparing plastinated EB for teaching, while highlighting some aspects related to plastination. Shrinkage of the nasal mucosa and the bony ethmoidal labyrinth was measured to see if tissue changes due to plastination modify endoscopic observations. The value of plastinated EB was examined for teaching by associating the reading of a CT-scan of the EB to the direct observation of the EB.

Materials and methods

Six cadavers were obtained from the local donation program at the Institute of Cell Biology and Morphology, University of Lausanne. Fresh human heads were used for the preparation of ethmoidal blocks according to the following protocol. The maxillary and internal carotid arteries were exposed, cannulated and

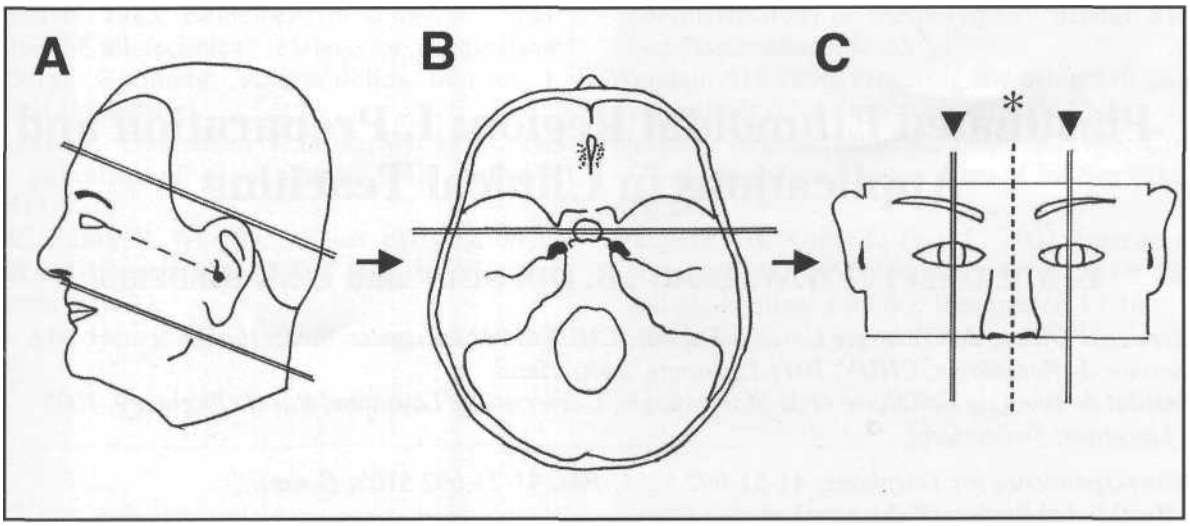

Figure 1. Preparation of the ethmoidal blocks with saw lines indicated and sequential procedure from A-C.

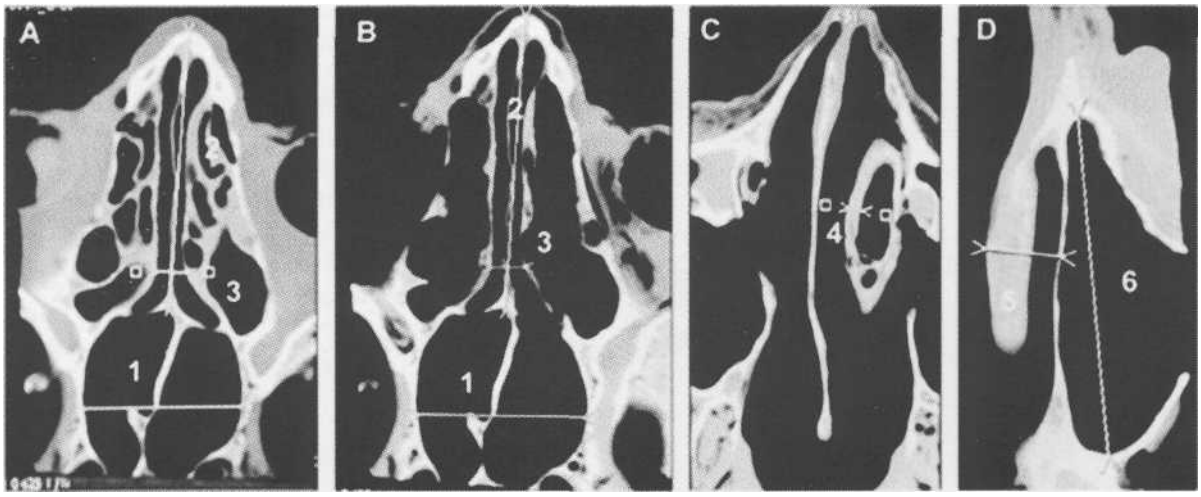

Figure 2. Axial CT-images of EB before (A) and after (B, C, D) plastination, demonstrating measurement sites. B. Specimen in A after complete ethmoidectomy and plastination. C. Middle left turbinate - Anatomical variation (concha bullosa). D. Sagittal axis of Maxillary sinus. 1. Intersphenoidal width, 2. Nasal bone to vomer heighth, 3. Width of posterior nasal fossa, 4. Mucosal thickness of medial wall of concha bullosa, 5. Intersinusonasal wall to medial side of inferior concha. 6. Sagittal axis of maxillary sinus.

	Parameter measured	Measurement before plastination	Measurement after plastination	Bone and mucosa shrinkage
1	Intersphenoidal width	27.9 mm	27.8 mm	0.36%
2	Nasal bone to vomer	49.3 mm	49.2 mm	0.2%
3	Width of posterior nasal fossa	5.3 mm	5.3 mm	0%
4	Mucosa - medial wall of concha bullosa	2.4 mm	2.3 mm	4.1%
5	Intersinusonasal wall to medial side of inferior concha	10.0 mm	10.0 mm	0%
6	Sagittal axis of maxillary sinus	43.8 mm	43.7 mm	0.23%

Table 1. Measurements from magnified CT-scans.

injected following the procedure of Musumeci and colleagues (2003). Heads were frozen at -20°C and sliced on a band saw horizontally into three pieces (Fig. 1A). The saw lines were parallel to a line joining the external acoustic meatus to the external (lateral) canthus of the eye (dotted line). The middle block was saved for preparation of the EB and allowed to thaw to remove the brain. After removal of the brain, the block was frozen again. Further block preparation was by sawing vertically through the middle of the sella turcica (Fig.IB) and by removing the external (lateral) quarters of the face by sawing along a line passing through the middle of the orbit (Fig. 1C). From the six heads, two remained as complete blocks, while four were separated into eight hemiblocks by sawing on the midline and removing the nasal septum (Fig. 1C). After sawing of the ethmoidal blocks, they were stored in 50% ethanol at room temperature to await the intended surgical dissection. Six frequent endoscopic sinus surgeries were performed on the ethmoidal blocks: antrostomy, unciformectomy, frontomeatotomy, anterior ethmoidectomy, posterior ethmoidectomy with sphenoidotomy and complete ethmoidectomy. On eight hemiblocks the following combinations of surgerical interventions were performed: two antrostomies; one antrostomy and unciformectomy; two antrostomies, unciformectomies and frontomeatotomies; one antrostomy, unciformectomy, frontomeatotomy and anterior ethmoidectomy; one posterior ethmoidectomy and sphenoidotomy; and on one hemiblock and two complete blocks, all six procedures were performed. An anterior middle turbinectomy was done to gain access to the middle meatus. A dissecting microscope and an endoscope were used for surgical interventions.

Multirow detector helical computer tomography (MRCT) was performed with a Lightspeed QX/i Scanner (GE Medical Systems, Milwaukee, Wis, USA). The scanning parameters used for MRCT were: 120 kVp, 200 mAs, FOV - 16, section thickness - 1.25mm, and image data was reconstructed at 0.7mm intervals. The reformatted images were transferred to a GE Advantage Workstation (version 4.0), where 2D coronal and sagittal views were obtained at 0.5mm intervals and photographed with a wide window width (3,500 UH) centered at +400 UH to enable precise analysis of the bony structures. CT-scans were made after surgery (while specimens were held in 50% alcohol) and after plastination using similar parameters. The following parameters were measured on magnified CT-scan images from each EB before and after plastination (Fig. 2): 1. Intersphenoidal width, 2. Nasal bone to vomer height, 3. Width of posterior nasal fossa, 4. Mucosal thickness of medial wall of concha bullosa, 5. Intersinusonasal wall to medial side of inferior concha, 6. Sagittal axis of maxillary sinus. These measurements are listed in Table 1.

Plastination of specimens was done using the standard S10 method (von Hagens, 1985; Henry and Nel, 1993; Weiglein and Henry, 1993). The steps taken and their associated time intervals were: dehydration was performed at room temperature using a graded series of technical alcohol of increasing concentrations from 50% to 100%, changed every third day with a final three changes in 100% ethanol. Ethanol dehydrated specimens were placed into 95% acetone at 4°C for 24 hours and then into 100% acetone at -20°C which was changed three times at three day intervals. Specimens were submerged in -20°C silicone polymer (10 Biodur®) containing 1% catalyst (S3 Biodur®) for 24 hours. The next day, vacuum was applied and impregnation was started by reducing air pressure gradually over a period of 4-5 days. After impregnation was complete, excess silicone was drained first at -20°C, then at room temperature. After draining, excess silicone was wiped off with gauze and paper towels before and during the early phases of curing with S6 (Biodur®). During curing, openings into cavities were filled with gauze to prevent pooling of polymer and ensure the openings of the nasal cavities remained patent to allow entry of the endoscope later. After curing, landmarks, which are delicate and crucial, were marked on several specimens with colored nail polish. These marks were coated with a silicone-mix and hardened.

Results

After curing, no morphological changes were observed and anatomical detail was still visible, even six months after plastination of the blocks. The plastinated concha were more rigid than the 50% alcohol fixed tissue. The shrinkage of the mucosa 6f the EB and the ethmoidal labyrinth was 0 to 5% (mean value: 2.3%) and 0 to 3% (mean value 1%) respectively during dehydration and plastination.

From the six heads, two were not separated and remained as complete blocks, while four were prepared into eight hemiblocks and the resultant specimens were of equal quality. Of the six surgical approaches utilized, the quality of the plastinated end products were similar. The vertical midline cut removed the anterior turbinate.

The EB in figure 3 demonstrates before and after surgical intervention of an unciformectomy, anterior ethmoidectomy and a frontomeatotomy. The anatomical changes produced by the surgery are easily seen, since the bony parts are missing. The anterior middle turbinectomy allowed easy access to the middle meatus.

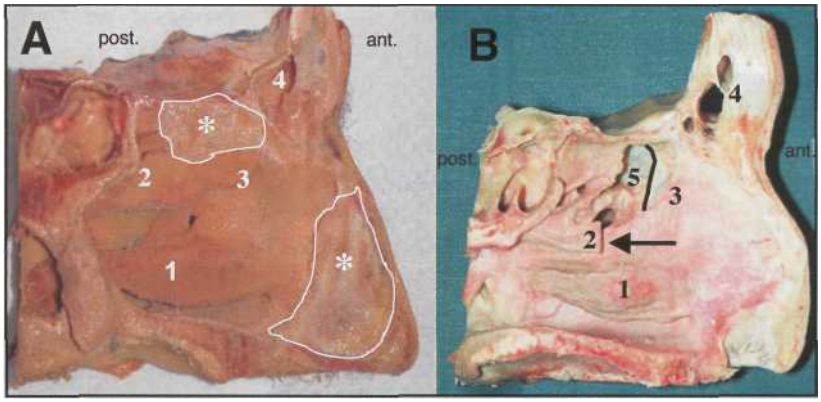

Figure 3. Left hemiblocks: A. Before surgery and plastination. B. After surgery (unciformectomy, anterior ethmoidectomy, frontomeatotomy) and plastination. 1. Inferior turbinate, 2. Middle turbinate, 3. Uncinate region, 4. Frontal sinus, 5. Hollow ethmoid bulla, * with white outline indicates remaining nasal septum.

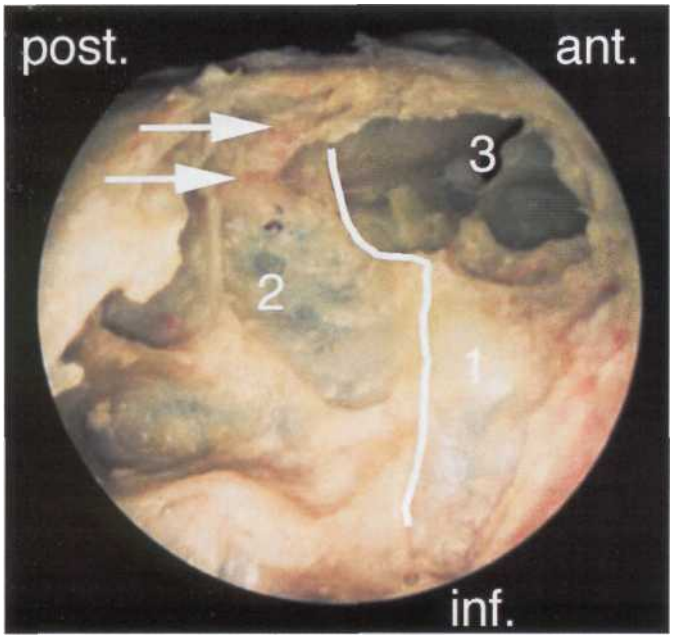

A **Figure 4.** Endoscopic view of left plastinated EB in Figure 3B. 1. Unciformectomy; 2. Anterior ethmoidectomy; 3. Frontomeatotomy. Arrows - Bony canal of anterior ethmoidal artery.

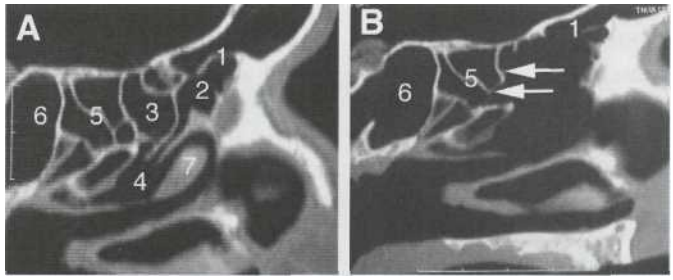

Figure 5. Sagittal CT-scans (Left hemiblock). A. Preoperative. B. Postoperative (Unciformectomy, Anterior ethmoidectomy and Frontomeatotomy). 1. Nasofrontal canal, 2. Uncinate process, 3. Anterior ethmoid cells, 4. Middle meatus, 5. Posterior ethmoidal cells; 6. Sphenoid sinus, 7. Middle turbinate, Arrows - Basal lamella of middle turbinate.

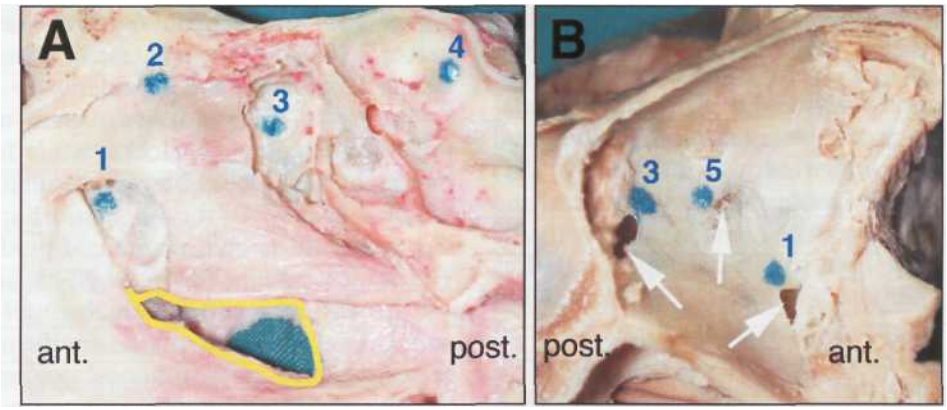

Figure 6: A. Plastinated right hemiblock, Medial view. Complete ethmoidectomy, antrostomy (yellow line), unciformectomy and sphenoidotomy. B. Plastinated right orbit with orbital bony breakages (arrows) in 3 weaker areas, Lateral view. Less resistant bony areas: 1. Lacrimal bone (uncinate process), 2. Cribriform plate, 3. Lamina papyracea of central posterior ethmoidal cells, 4. Anterior wall of optic canal in sphenoid sinus, 5. Lamina papyracea of bulla.

Tridimensional rhinosinusal anatomy is shown in figures 4 and 5. For each dissected block, pre- and postoperative CT-scans provided a three-dimensional correlation of the radiographic anatomy (Fig. 6). Vascular injection of the internal carotid, ophthalmic and ethmoidal arteries via the maxillary artery highlighted the vessels so that they were visible to the naked eye as well as radiographically. The marking of the less resistant bony areas of the ethmoidal labyrinth was also clearly visible.

Discussion

This work demonstrated that plastination with the S10 standard method described by von Hagens (1985) is applicable for preparing human EB. However, we recommend using the described cutting lines (Fig. 1) to make a useful block. The resection of the head of the middle turbinate was done prior to plastination to gain access to the ethmoid, because the post mortem specimen doesn't offer the same tissue elasticity as the living patient. The absence of the anterior turbinate also helps visualize the underlying ethmoidal surgery. Unciformectomy, anterior ethmoidectomy and frontomeatotomy consist of hollowing out the uncibullar complex and enlarging the nasofrontal canal, absolutely respecting the lamina papyracea and the ethmoidal roof. It is evident that the blocks allow a better comprehension of the difficult tridimensional anatomy of the sinus and show in a glance what must be the result of such an operation.

Sinus plastination has been performed and published using the entire EB *in situ* of birds (Henry et al., 1997) and axial slices of human sinuses (Sprinzl et al., 1995) for purely descriptive purposes. A recent publication by Durand and coworkers (2001) provides an example of a plastinated model of maxillary sinuses that was used to test aerosols.

Although the standard S10 procedure described by von Hagens (1985) was used, there are several key points worth mentioning. Before curing, it was important to drain and wipe off any excess silicone in order to obtain empty sinus cavities. As well, to keep the nasal cavity, sinuses and openings free of polymer and open, it was important to fill spaces and openings with gauze and change as needed.

The plastination of EB presents numerous advantages. The blocks are odorless, dry, reusable, more robust and durable for years. Furthermore, because shrinkage of the nasal mucosa or of the ethmoid labyrinth could change nasosinus anatomy and endoscopic observation, pre and post plastination measurement of the bone and mucosa were recorded. We observed that the average bony and mucosal shrinkage was small (1% and 2.3%, respectively). In previous studies, tissue shrinkage in plastination was reported to vary between 8.2-29% (Brown et al., 2002). These values are quite different from those reported here, but Brown and colleagues reported results from kidney, liver and hearts from various species, while we focused on bony structures. This can easily explain a difference in shrinkage. Thus, plastination does not significantly shrink or distort the EB, and endoscopic appearance remains fairly realistic. Nevertheless, the loss of natural elasticity due to this technique makes endoscopic observation slightly more difficult.

For trainees in otorhinolaryngology, learning surgical techniques (especially those techniques associated with endoscopic sinus surgery) is critical to understand the regional anatomy because complications, although rare, can have disastrous consequences (May et al., 1994; Sharp et al., 2001). Surgical intervention is often required when conservative treatment of chronic infectious sinusitis, nasal polyposis, mucocoele or acute sinusitis fails. These six techniques (antrostomy, unciformectomy, frontomeatotomy, anterior ethmoidectomy, posterior ethmoidectomy with sphenoidotomy and complete ethmoidectomy) demonstrated on EBs are the most common procedures performed in endoscopic sinus surgery. Anatomical study of an EB with the naked eye or microscope, combined with endoscopic observation gives an excellent tridimensional view of the operative principles and their limits. Moreover, by marking less resistant bony areas of the ethmoidal labyrinth, areas for potential surgical complications are highlighted and areas that must always be preserved are pinpointed. Awareness of areas of potential operative complications was aided by injecting the internal carotid and maxillary arteries with a substance that rendered the regional vessels visible to the naked eye as well as radiographically (Musumeci et al., 2003) and by marking with colored nail polish the less resistant bony areas of the ethmoidal labyrinth (Waridel et al., 1997). These spots of color were coated with a thin film of silicone to increase their resistance to mechanical insult (Fig. 6). The optic canal, the wall of which has a resistance three times greater to the most fragile bony areas of the labyrinth, is not represented in figure 6. Nevertheless, breaking of the anterior wall of the optic canal with a resulting lesion of the optic nerve is one of the most serious complications of endoscopic sinus surgery (May et al., 1994). These marked areas alert the physician during endoscopic training to use caution when approaching these delicate areas of the plastinated nasal cavity.

The use of the endoscopic and CT-scan observations

enhanced the study of tridimensional rhinosinusal anatomy and allowed the different steps of the surgery to be followed easily. The study of plastinated EB gives a more realistic understanding of ethmoidal anatomy and adds a tool that seems superior to books of clinical, radiographic and tridimensional rhinosinus anatomy, including its numerous variations and optic nerve and internal carotid artery precautions. Although the higher rigidity of plastinated tissue rendered endoscopic observations of EB slightly more difficult. EB in clinical teaching may be used in surgery, endoscopy and radiology. The training on ex vivo specimens (EB) remains fundamental. However, the use of plastinated EB should simplify and shorten the training phase and contribute to diminishing the number of cadaver heads needed for the apprenticeship of endoscopic sinus surgery and in the future decrease potential surgical complications.

Since sinus surgery is currently performed primarily using endoscopy, it is very important that the plastinated EB can also be examined endoscopically.

Acknowledgements: The authors thank Profs. P. Monnier and F.P. Harris for their constructive comments. This work was supported by the IBCM. The first author thanks his wife and children for their moral support.

Literature cited

Brown MA, Reed RB, Henry RW. 2002: Effects of dehydration mediums and temperature on total dehydration time and tissue shrinkage. J Int Soc Plastination 17:28-33.

Durand M, Rusch P, Granjon D, Chantrel G, Prades JM, Dubois F, Esteve D, Pouget J-F, Martin C. 2001: Preliminary study of the deposition of Aerosol in the maxillary sinuses using a plastinated model. J Aerosol Med 14:83-93. Henry RW, Antinoff N, Janick L, Orosz S. 1997: El 2 Technique: an Aid to Study Sinuses of Psittacine Birds. Acta Anat 158:54-58. Henry RW, Nel PPC. 1993: Forced impregnation for the standard S10 method. J Int Soc Plastination 7(1):27-31. May M., Levine H. L., Mester S. J., Schaitkin B. 1994: Complications of Endoscopic Sinus Surgery: Analysis of 2108 Patients - Incidence and Prevention. Laryngoscope 104:1080-1083. Musumeci E, Lang FJW, Duvoisin B, Riederer BM. 2003: Plastinated ethmoidal region: II. The preparation and use of radio-opaque artery casts in clinical teaching J Int Soc Plastination 18:29-33. Sharp HR, Crutchfield L, Rowe-Jones JM, Mitchell DB. 2001: Major Complications and Consent Prior to Endoscopic Sinus Surgery. Clin Otolaryngol 26:33-38. Sprinzl GM, Eckel HE, Sittel C, Thumfart WF, Koebke J. 1995: Ganzorganplastination in der Hals-Nasen-Ohrenheilkunde. HNO 43:282-286. Stammberger H, Posawetz W. 1990: Functional Endoscopic Sinus Surgery. Eur Arch Otolaryngol 247:63-76. Stankiewicz, JA. 1987: Complications of Endoscopic Intranasal Ethmoidectomy. Laryngoscope 97:1270-1273. von Hagens G. 1985/1986: Heidelberg Plastination Folder. Anatomisches Institut I, Universitat Heidelberg, D-6900 Heidelberg. Waridel F, Monnier P, Agrifoglio A. 1997: Evaluation of the Bone Resistance of the Sphenoid and Ethmoid Sinuses. Laryngoscope 107:1667-1670. Weiglein A, Henry RW. 1993: Curing (Hardening, Polymerization) of the polymer - Biodur S10. J Int Soc Plastination 7(l):32-35.

Journal of the International Society for Plastination 18:29-33 (2003)

Plastinated Ethmoidal Region: II. The Preparation and Use of Radio-opaque Artery Casts in Clinical Teaching

E. MUSUMECI[1], F.J.W. LANG[1], B. DUVOISIN[2] and B.M. RIEDERER[3]*

'Service d'ORL etde Chirurgie Cervico-Faciale, CHUV, 1011 Lausanne, Switzerland.
'Service de Radiologic, CHUV, 1011 Lausanne, Switzerland.
[3]Institut de Biologie Cellulaire et de Morphologie, Universite de Lausanne, Rue du Bugnon 9, 1005 Lausanne, Switzerland.

* *Correspondence to: Telephone:* 41-21-692 5154, *Fax:* 41-21-692 5105; *E-mail:* BeatMichel.Riederer@ibcm.unil.ch

Abstract: In endoscopic sinus surgery, knowledge of the course of the internal ethmoidal and orbital arteries is crucial. The maxillary and the internal carotid arteries of cadavers were injected with radio-opaque, red colored silicone. The ethmoidal regions were prepared and plastinated using the standard S10 technique. On some specimens, the ophthalmic and ethmoidal arteries were dissected prior to plastination. The plastinated specimens of the ethmoidal blocks were successfully introduced into clinical teaching of sinus anatomy and surgery as an aid to study vascularization and its relationship to surgical procedures. Among the advantages of this method are the long-lasting preservation of dissected tissue, visualization of arteries during endoscopic and radiological examinations, and invaluable teaching and training resources for endoscopic sinus surgery.

Key words: **anatomy; endoscopy; plastination; radiology; sinus; surgery**

Introduction

Knowledge of the exact location of the orbital and internal carotid arteries is crucial when performing endoscopic sinus surgery. In fact, injury of one of these arteries can provoke life-threatening hemorrhage from the nose or in the orbit or brain, which can lead to permanent damage despite emergency operative measures. In order to perform such surgery, it is necessary that surgeons train on cadaveric material. In this study, arteries of the ethmoidal region were injected with radio-opaque, colored silicone and ethmoidal blocks (EB) were prepared. After EB were prepared, the arteries were dissected to provide better visualization. Plastination was chosen to permanently preserve the injected EB. The plastinated EB help provide an understanding of various surgical procedures and potential complications that can occur when arteries are damaged. The advantages of plastinated EB for teaching are reported. Special reference is given to visualizing the ophthalmic and ethmoidal arteries on anatomical preparations using the naked eye, the endoscopic and radiographic techniques.

Materials and methods

Cadavers with prior written consent were obtained from the local donation program at the Institute of Cell Biology and Morphology. For the preparation of casts, fresh heads, which are better than embalmed tissue, were used. A mixture of radio-opaque, colored silicone was prepared from 57% dense silicone (Elastosil® M 4500, Wacker-Chemie GmbH, 81737 München, Germany), 40% silicone oil (AK 50®, Wacker-Chemie GmbH, 81737 München, Germany) and 3% hardener (Wacker T12®, Drawin Vertriebs-GmbH, 85521 Ottobrunn, Germany). To this solution, 3% red pigment

(SAL 300®) and 5% lipophil iodized solution (Lipiodol® ultra-fluid = Ethiodol® in the USA; Laboratoire Guerbet, 93600 Aulnay-Sous-Bois, France) were added. In order to determine homogeneity of this radio-opaque solution of silicone, mixtures of varying concentrations (50, 25, 10, 5, 1%) of Lipiodol were prepared and placed in 1.2mm id catheters and evaluated visually and radiographically.

After the best concentration of radio-opaque, colored silicone was determined, the heads were injected with 5% Lipiodol used to make the colored, radio-opaque silicone solution. The left and right maxillary and internal carotid arteries were exposed and catheterized with flexible plastic tubing (2mm id). These arteries were filled with 100 to 200ml of the silicone solution using 60ml syringes attached to the tubing. Because of vascular resistance and the viscosity of the solution, injection time was rather long (8 to 10 minutes). Hence, a syringe equipped with a common caulking gun was used to decrease injection time and assure vascular filling. Filling was stopped when the solution came out of the internal jugular vein and the anterior and posterior spinal veins. This caulking is available in do-it-yourself shops or hardware stores and makes injection easier and forceless.

After injection, the heads were stored in a refrigerator at 4°C for two days while the silicone hardened. After the silicone mix hardened, the heads were frozen at -20°C and cut with a band saw following the protocol described by Musumeci and coworkers (2003). The brain was removed and the block was frozen again. The ethmoidal blocks were cut and kept in 50% ethanol at room temperature during preparation of the surgical interventions and performing CT scans of the EB. A CT-scan was performed prior to surgical intervention with a Lightspeed QX/i Scanner (GE Medical Systems, Milwaukee, WS, USA). The scanning parameters used for multi-detector row CT were: 120 kVp, 200 mAs, FOV - 16, section thickness 1.25mm and image data were reconstructed at 0.7mm intervals. The reformatted images were transferred to a GE Advantage Workstation (version 4.0). At the workstation, 2D coronal and sagittal views were obtained at 0.5mm intervals and imaged with a wide window width (3,500 UH) and centered at +400 UH to enable precise analysis of the bony structures. To evaluate the opacified ethmoidal and ophthalmic arteries 3D images were reconstructed from the coronal and sagittal views using the volume rendering reformatting technique, which incorporates all relevant data into the resulting image. The vessels were colored red using Adobe Photoshop. A dissecting microscope and an endoscope were used for performing the various surgical interventions, such as unciformectomy, frontomeatotomy, ethmoidectomy or antrostomy and dissection of the orbital arteries. CT-scans were also performed after surgery and after plastination using the same parameters as described before. After the surgeries were completed, the specimens were plastinated using the classic cold S10 technique (von Hagens, 1985; Henry and Nel, 1993; Weiglein and Henry, 1993). CT scans were taken once again after plastination using the same parameters as above.

Results

All percentages of the radio-opaque silicone solutions made from 5% Lipiodol as well as pure Lipiodol were visible in the 1.2mm diameter tubes with the eye and on CT scan (Fig. 1). The concentrations of 50% and 25% of Lipiodol® did not remain homogenous. The 1 % solution showed less radio-opacity and was less visible than the 5 and 10% solutions.

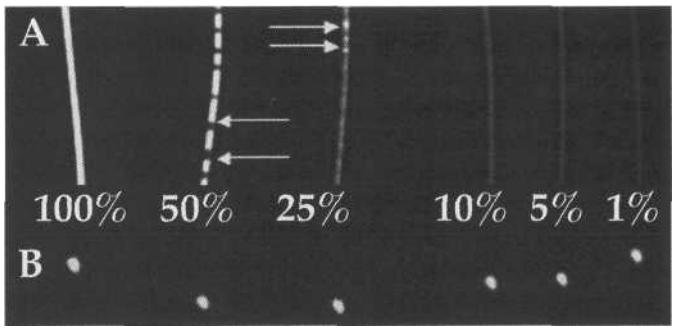

Figure 1. Longitudinal (A) and transverse (B) CT-scan of 1.2mm diameter plastic tubes filled with decreasing % concentrations of Lipiodol® in a colored silicone solution. Arrows - Uneven distribution of silicone and Lipiodol.

Injection of the radio-opaque colored silicone resulted in good opacification of the orbital and internal carotid arteries in all four cadaver heads (Figs. 2, 3). As well, the injected arterioles, veins, and capillaries of the skin and mucosa of the hemiblocks were red (Figs. 2, 3, 4). The difference in the tissue color between an injected and non-injected ethmoidal block (EB) is demonstrated in Figure 2.

After injection and prior to dissection, the trajectories of the ophthalmic, anterior and posterior ethmoidal and internal carotid arteries were visible on the three dimensional CT-scan reconstructions (Fig. 4). After dissection of the orbital arteries and after anterior and posterior ethmoidectomy, all arteries could be seen with the naked eye, radiographically and endoscopically (Figs. 4, 5). The arteries of the orbit, the stump of the optic nerve, the ophthalmic and the supratrochlear arteries are recognizable, as well as the anterior ethmoidal artery with its entry in the lamina papyracea. In one ethmoidal block, aggregation of color was noted

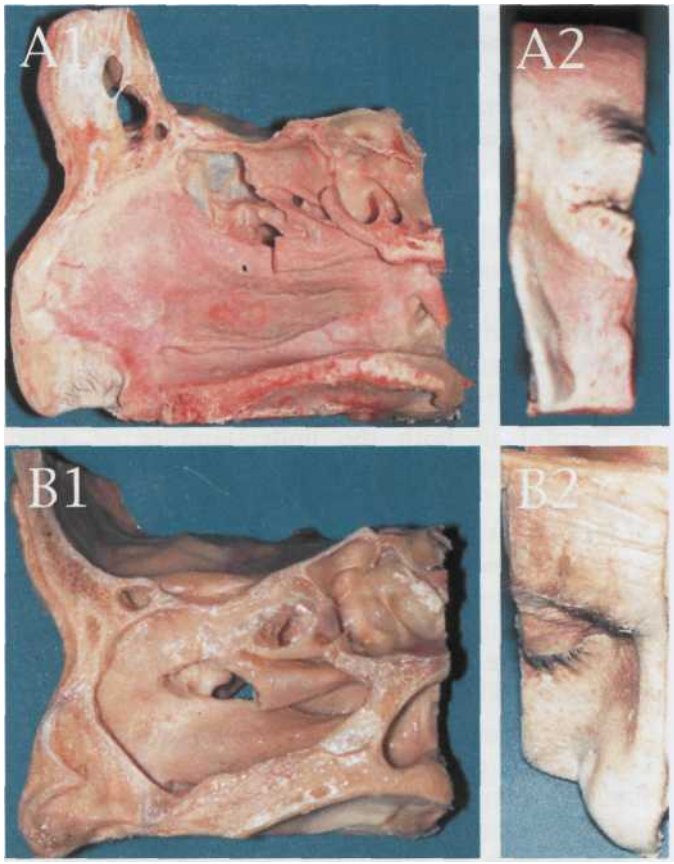

Figure 2. Plastinated and operated hemiblocks: A (color injected), B (not injected); 1. Sagittal view, 2. Frontal view.

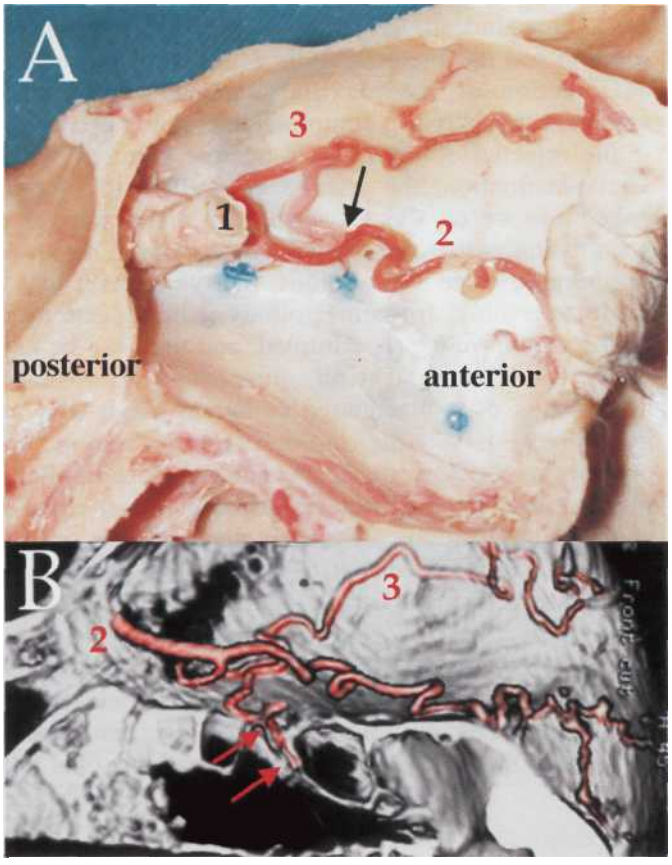

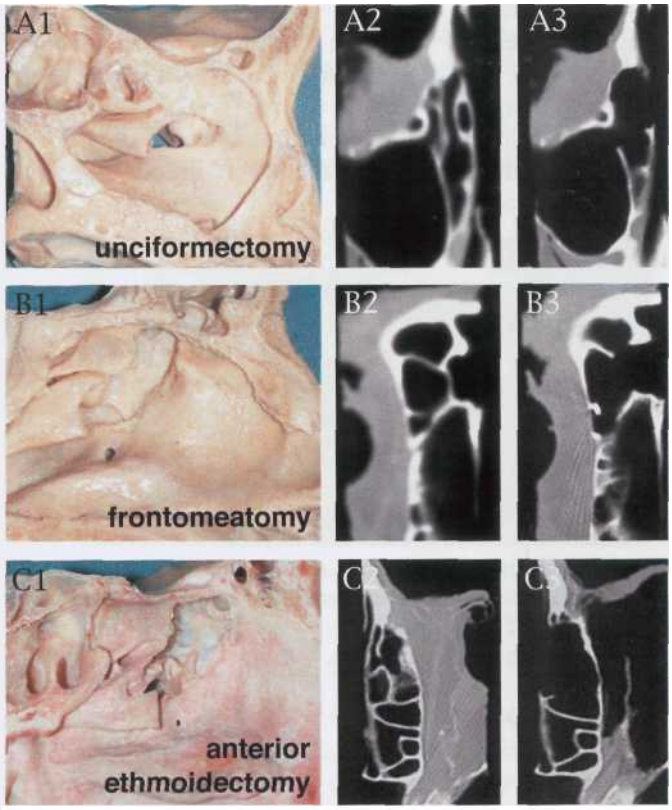

Figure 3. Correlation of specimen (1) and axial CT-scans: Pre-surgery (2), Post-surgery (3). Surgical interventions: A. Unciformectomy, B. Frontomeatomy, C. Anterior ethmoidectomy,

A **Figure** 4. A. Lateral view of orbit. B. 3D reconstruction of CT-scan axial view of the orbital cavity. The upper part represents the orbit and the lower part the ethmoid. The optic nerve is not visible on the reconstruction and the arteries were colored using Adobe photoshop. 1. Optic nerve, 2. Ophthalmic artery, 3. Supratrochlear artery, Black arrow - Entrance of anterior ethmoidal artery into the lamina papyracea, Red arrows - Anterior ethmoidal artery on the ethmoidal roof.

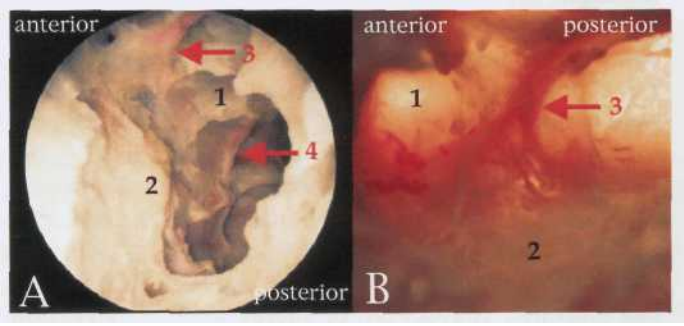

Figure 5. A. Endoscopic view of an EB after complete ethmoidectomy. B. Endoscopic view with transillumination of the ethmoidal block roof. 1. Ethmoidal roof, 2. Lamina papyracea, 3. Anterior ethmoidal artery in its bony canal, 4. Posterior ethmoidal artery in its bony canal.

after plastination (Fig. 6). The color enhancement of the reconstructed 3D images from the CT scans rendered the vessels quite prominent such that the anterior ethmoidal artery is seen on the roof of the ethmoid (Fig. 4B). Transillumination of ethmoidal roof on EB (Fig. 5B) aided identification of the thin ethmoidal arteries in their bony canals.

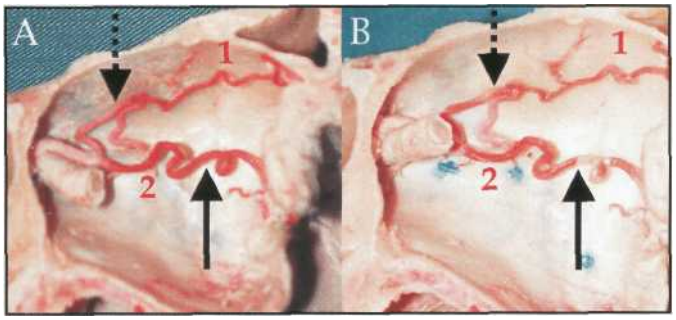

Figure 6. Lateral views of orbit: A. Before plastination, B. After plastination. 1. Supratrochlear artery, 2. Ophthalmic artery, Solid and dotted arrows - Sedimentation of the colored, radio-opaque solution.

Discussion

Vascularization of the ethmoidal sinus region is of clinical relevance and must be known before practicing endoscopic sinus surgery. Hemorrhages, such as orbital hematomas (pre- and postseptal), epistaxis after sinus surgery and focal brain hemorrhage, represent a large percentage of minor and major complications (Stankiewicz et al., 1987; May et al., 1994). Epistaxis can be cataclysmic after injury of the internal carotid artery. In a recent study, Sharp and colleagues (2001) reported that the incidence of major and minor hemorrhagic complications represented 0.04% and 0.44% of all endoscopic sinus interventions, respectively. Knowledge of the trajectories of the ethmoid, sphenopalatine and internal carotid arteries is therefore primordial for successful prevention of potential hemorrhagic complications.

An iodinated colored silicone solution was needed to highlight the vessels of the region so that the vessels could be seen by eye as well as radiographically. It was necessary to determine the percent of iodine needed. Of the 5 mixtures with silicone compounded and the one pure solution, 5% Lipiodol® solution was chosen to highlight the vessels as it was visible in the thin (1.2mm) tubing, remained a homogeneous solution, and did not interfere with the hardener of the silicone. Concentrations of 50% and 25% of Lipiodol® were not stable and did not remain homogeneous. However, with macroscopic, endoscopic or radiographic observations the vessels were still distinguishable.

After injecting cadaver heads with the colored, radio-opaque solution, dissecting the orbit, and splitting the ethmoidal block in two hemiblocks, the arterial vascularization of the medial wall of the orbit and of the ethmoid are clearly demonstrated. Although the ethmoidal arteries have a diameter of less than lmm, they were always recognizable by visual or endoscopic inspection. If necessary, transillumination of the EB can enhance the contrast of the injected arteries and improve observation and learning of surgical anatomy. After plastination, uneven coloration of arteries was observed in one ethmoidal block, probably due to accumulation and aggregation of injected material during the plastination process.

The use of arterial casts with a radio-opaque solution is helpful in both the understanding of arterial vascularization and allowing surgeons to be trained more easily. It facilitates the study of the relationships of the arteries to other anatomical structures and allows a comparison with the CT scans which are usually performed prior to endoscopic sinus surgery. The reddish color of the facial skin and nasal mucosa illustrates the excellent quality of the injection which also enhances the aesthetics of the EB.

Study of ethmoidal blocks should be recommended in a surgical training program before execution of the first surgical exercises on a cadaveric ethmoidal block. For this reason, plastination is especially useful because it makes such an anatomic preparation permanent and reusable for multiple training courses even though preparation of an injected and plastinated block is time consuming. Indeed, the preparation of the radio-opaque solution and the anatomical dissection are easy, as well as injection of the maxillary and internal carotid arteries, especially if a compression pistol is used. Even if the injected colored, radio-opaque solution settles after plastination, the arteries are still visible by the naked eye or on the CT-scan. The disadvantages of plastination is that the plastinated blocks are no longer re-operable once the various interventions such as unciformectomy, frontomeatotomy, ethmoidectomy or antrostomy have been performed, and they can be used only for demonstration purposes. Endoscopic observation of a plastinated complete block (but not hemiblock) is a little more difficult than *in vivo* observation, because the specimens are more rigid after plastination. However, the results of the most common surgical interventions are clearly demonstrable on both the plastinated EB and on CT-scans and serve as an excellent teaching and training tool.

Acknowledgments: The authors would like to thank Profs. P. Monnier and F.P. Harris for their critical comments. The authors thank for the institutional support of the IBCM. The first author thanks his wife

Journal of the International Society for Plastination 18:34-36 (2003)

Dry Preservation of Cadaveric Hearts: An Innovative Trial

S. MEHRA*, R. CHOUDHARY and A. TULI

Department of Anatomy, Lady Hardinge Medical College, New Delhi, India.

**Correspondence to: Telephone:* 011-5595616; *Fax:* 011-6848007; *E-mail:* ambuja42@rediffmail.com

Abstract: Decay is a vital process in nature but an impediment to morphological studies, teaching and research. It has always been a goal for anatomists to find suitable preservation techniques. Wet cadaveric specimens allow 'hands on' learning but students and teachers have to contend with noxious formalin fumes. This paper describes an alternative approach to the study and teaching of gross anatomy of human hearts to undergraduate and postgraduate students using Quickfix® impregnated dry cadaveric hearts. Formalin fixed hearts were utilized as the source of specimens to be plastinated. The reasons for this choice were a result of the decreased cadaveric availability and limited funds in our institution. The procedure is simple to perform, cost effective and carried out at room temperature (37°C-40°C). It precludes the use of expensive resins and equipment. The hearts were well preserved in the dry state without showing any change of color or fungal growth. We regard this process as an important factor in bridging the gap between anatomy and clinical practice.

Key words: **anatomy; cadaveric hearts; dry preservation; education; low cost**

Introduction

Reduction in clock hour allotments to the study of anatomy in the MBBS curriculum in our country necessitates an increased emphasis on teaching with the help of preserved, prosected specimens. Formalin fixed anatomical specimens are traditionally displayed in glass jars immersed in 10% formaldehyde. These are questionable teaching tools as the formaldehyde jars are fragile and immersion in fluid makes viewing difficult. They may be removed for observation but handling is unpleasant because of formaldehyde fumes. Also, on exposure to air, such specimens quickly lose color and their surface features progressively deteriorate. Dry preservation of cadaveric specimens is an alternative to formalin preservation. Plastination, a widely recognized technique for preserving biological tissue, was invented by von Hagens (1979). This procedure produces dry, odorless, durable and manipulative specimens. A number of innovations of von Hagens techniques have been tried by several investigators (Bickley et al., 1981; Tiedeman and von Hagens, 1986; Romero-Sierra et al., 1986; Updike and Holladay, 1986). All these require use of expensive resins and equipment. Keeping in view our limited financial resources and the high import cost of chemicals, the present study describes the use of locally available adhesives and chemicals for dry preservation of formalin fixed anatomical specimens with particular reference to human hearts. The technique (Janakiram et al., 1993) used in the present study has so far not been tried on whole visceral organs like heart. Such specimens complement existing teaching initiatives in a variety of disciplines from general biology courses through specialized courses in pathology, forensic medicine, oncology and are of great benefit to research.

Materials and methods

Twelve formalin fixed adult human cadaveric hearts were washed under running tap water to clean and remove blood clots. Excess water was squeezed out and the surface of the heart was wiped dry with a sponge. **In**

six hearts, the mitral and tricuspid valves were displayed using classic dissection procedures. Specimens were then immersed in an undiluted solution of commercial grade acetone for one week to remove tissue water. They were then removed from the acetone and suspended from hooks to be dried for 24 hours in a well ventilated room. A solution comprising equal parts of Quickfix® (Wembley Laboratories) and amylacetate was then prepared in glass jars large enough to hold two specimens. Specimens were immersed in this solution for a period of three months. The glass jars were sealed airtight. The specimens were taken out and suspended to be dried for 24 hours. The surfaces of the specimens were then coated with a fresh solution of Quickfix® (50% by volume) in amyl acetate with a fine brush and allowed to dry before being kept in the departmental museum for display. This procedure was repeated using varying dilutions of Quickfix® (60% v/v and 40% v/v) in amyl acetate against a fixed volume of amyl acetate. These techniques were carried out at room temperature (37°C to 40°C).

Results

The finished specimens were best in the trial utilizing equal amounts of Quickfix® and amyl acetate. The hearts were dry, hard to the touch and dark in color with a fine polished appearance (Fig. 1). The atrioventricular valves were translucent with clarity of detail (Fig. 2). There was good contrast between structures. The chordae tendinae were flexible. The rough and clear zones of the valve cusps were distinctly visualized against natural light. Even after three years, we have not found any deterioration of the specimens nor any color changes. Additionally, we have noted no fungal growth on the specimens.

Discussion

As more and more emphasis is placed on the use of prosected specimens to support teaching and learning of gross anatomy, and with the limited supply of finances and cadavers in our institution, we have tried to preserve cadaveric hearts using, non expensive and locally available chemicals like Quickfix®, amyl acetate and acetone. Prolonged exposure to Quickfix® and amyl acetate solution achieves adequate tissue penetration of the adhesive without the need of vacuum embedding as with von Hagens' plastination technique. Quickfix® alone is highly viscous and requires an equal amount of solvent to attain the desired viscosity to penetrate the deeper areas of the hearts. The proportion of equal volumes of Quickfix® and amyl acetate was found to be ideal in this study as is also reported by Janakiram et al. (1993) in their plastinated hand specimens. A certain degree of shrinkage was observed in the finished specimen. This, however, does not alter the gross relationships of the various structures within the specimen. Trials involving higher dilutions with solvents caused inadequate penetration of the specimens with marked shrinkage and rigidity.

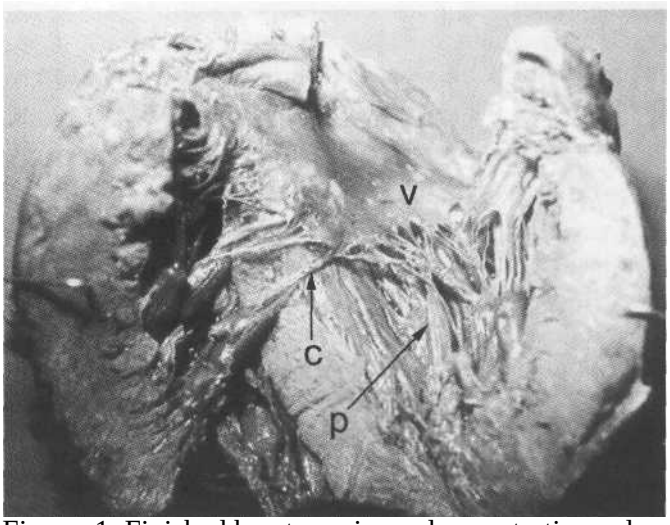

Figure 1. Finished heart specimen demonstrating valve leaflet (v), chorda tendineae (c) and papillary muscle (p).

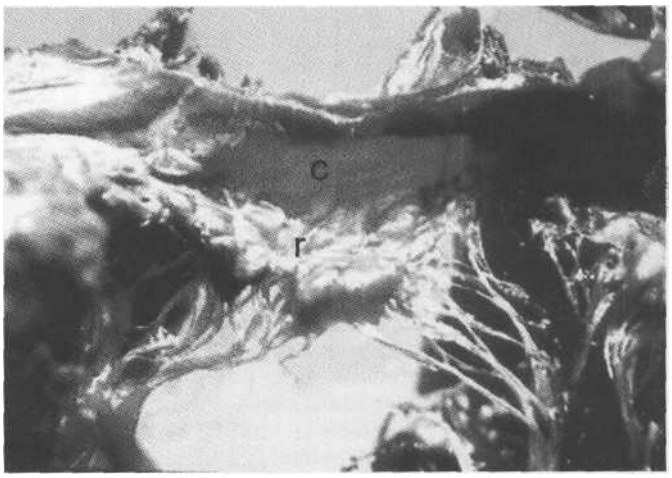

Figure 2. View of valve leaflet demonstrating the clear (c) and rough (r) zones.

Specimens preserved by this method are much lighter than their wet counterparts. They are non-toxic and durable despite the day to day handling. This technique has been reported (Janakiram et al., 1986) to preserve thin slices (100 microns) of gross specimens like lung, liver and heart in a dry state. Quickfix® has been used as a mounting medium in histology studies (Victor et al., 1988). To date, the technique described here has not been reported to be used for preserving whole visceral organs like the heart. The technique of heart plastination described by Tiedemann and von Hagens (1982) involves the use of special equipment

and expensive resins. In contrast, the technique followed by us is cost effective, simple to perform, precludes the use of costly equipment and stringent temperature requirements. These new and unique teaching aids preserve the anatomical details observed during dissection. Such specimens are of obvious use in teaching anatomy courses that comprise a multimedia approach utilizing wet specimens, plastic or plaster of pans models, radiographs, diagrams and computers.

Literature cited

Bickley HC, von Hagens G, Townsend FM. 1981: An improved method for the preservation of teaching specimens. Arch Pathol Lab Med 105:674-676.

Janakiram S, Balasubramanyam V, Victor R, Thomas IM. 1993: Dry preservation of cadaveric material: An indigenous trial. J A S 142(2):95-97.

Janakiram S, Victor R, Kamath S, 1986: Plastic mounted sections for teaching and museum display. J ASI36(1):71.

Romero - Sierra C, Webb JC, Lyons GW, Desmarteau JK, Carlson KC. 1986: Preparation of freeze dried hearts for use as teaching aids. Collection Forum 2(2):11-13.

Tiedemann K and von Hagens G. 1982: The technique of Heart plastination. Anat Rec 204:295-299. Updike SJ and Holladay SD. 1986: Preparation of flexible models of hollow gastrointestinal organs. Anat Rec 216:207-210. Victor R, Janakiram S, Chinamma KC, Kamath S. 1988: Plastic mounting of histological sections for teaching and display. Clinician 52(6): 162-164. von Hagens G. 1979: Impregnation of soft biological specimens with thermosetting resins and elastomers. Anat Rec 194:247-256.

and children for their moral support.

Literature cited

Henry RW, Nel PPC. 1993: Forced impregnation for the standard S10 method. J Int Soc Plastination 7(1):27-31.

May M, Levine HL, Mester SJ, Schaitkin B. 1994: Complications of Endoscopic Sinus Surgery: Analysis of 2108 Patients - Incidence and Prevention. Laryngoscope 104:1080-1083.

Musumeci E, Lang FJW, Duvoisin B, Riederer BM. 2003: Plastinated ethmoidal region: I. Applications in clinical teaching and effects of tissue shrinkage. J Int Soc Plastination 18:23-28.

Sharp HR, Crutchfield L, Rowe-Jones JM, Mitchell DB. 2001: Major Complications and Consent Prior to Endoscopic Sinus Surgery. Clin Otolaryngol 26:33-38. Stankiewicz JA. 1987: Complications of Endoscopic Intranasal Ethmoidectomy. Laryngoscope 97:1270-1273. von Hagens G. 1985/1986: Heidelberg Plastination Folder. Anatomisches Institut I, Universitat Heidelberg, D-6900 Heidelberg. Weiglein A, Henry RW. 1993: Curing (Hardening, Polymerization) of the polymer - Biodur S10. J Int Soc Plastination 7(l):32-35.